Archean Rocks unraveled: an ‘exclusive’ first impression on paleomagnetism of deep-drilled rocks of the Onverwacht Suite, Barberton Greenstone Belt (SA)

K.A. Dijkhuizen, October 2011

Paleomagnetic Laboratory ‘Fort Hoofddijk’, Utrecht University, Budapestlaan 17, 3584 CD Utrecht, The Netherlands

Abstract

Rocks from the 3.5-3.1 Ga Barberton Greenstone Belt (BGB), South Africa, may provide information about the earliest history of our Earth. In this period, early life started, plate tectonics as we know today may have started and a stable geomagnetic field could already have been in place. To get constraints on the Early Earth’s tectonics and geodynamo behaviour and development, paleomagnetic data on these Archean rocks are necessary. Previous studies on surface rocks indicate a great potential for rocks from the Onverwacht Suite of the BGB. (Near) primary geomagnetic signals indicate the presence of a stable geomagnetic field during this period. However, surface rock data are not straightforward since surface processes like lightening and weathering influence the primary signal in rocks. In 2009, the Barberton Scientific Drilling Program (BSDP) started drilling inside the BGB in a large folded structure: the Onverwacht Anticline. This study describes the first paleomagnetic research on these fresh rocks throughout the whole cored section. Despite large low temperature or low coercive overprint components, most likely caused by (re)magnetization of the core by the equipment used for cutting, data from samples of the Hooggenoeg Complex indicate the presence of a possibly (near-) primary signal. Comparison with recent studies on similar rocks from outcrops, however, gives incompatible result. Nevertheless, the new paleomagnetic data from this study support the hypothesis of the presence of a stable geomagnetic field during the mid-Archean.

1 Introduction

1.1 Archean Rocks and the Barberton Scientific Drilling Program

Mid-Archean rocks are rare but can be found at several sites scattered around Earth's surface. Rocks from the Barberton Greenstone Belt (BGB) in South Africa and the Pilbara Craton in northwestern Australia have been the focus of various paleomagnetic studies on Archean rocks because of their low grade of metamorphism (O'Nions & Pankhurst, 1978). To understand the processes during this very early stage in Earth's history it is important to investigate the presence of a geomagnetic field during the Achean. With paleomagnetic research answers can be found for questions concerning Early Earth's core behaviour and the nature of an early geomagnetic field. Surface studies on Archean rocks of the Barberton Greenstone Belt (BGB) have addressed several uncertainties concerning the physical, chemical and biological aspects acting on the Early Earth (cf. Grosch *et al.*, 2009). From earlier studies it is known that the rocks from the BGB are promising for paleomagnetic studies (e.g. Biggin *et al.*, 2011) and for studies on the beginning of life on Earth by the recognition of bacteria (e.g. Furnes *et al.*, 2004). The Barberton Scientific Drilling Program (BSDP) was therefore initiated to drill three holes in the rocks of the BGB (Figure 1) for an advanced study on particular early life (see Grosch *et al.*, 2009 for an overview).

In this study, paleomagnetic data of these deep-drilled rocks will be presented. Since surface processes like lightening and weathering have acted for many years on exposed rocks, studies can be better performed on fresh rock. Therefore, it is expected that paleomagnetic signals from the deep-drilled rocks are more straightforward compared to data from surface rocks. The main objective is to construct a paleomagnetic framework for rocks from the Onverwacht Group to investigate the paleomagnetic behaviour of these rocks. Focus will be on paleomagnetic data to critically assess the outcome of other studies (Usui *et al.*, 2009; Biggin *et al.*, 2011) that some rocks from the BGB are likely to record (near) primary magnetization signals.

Since the study on early life is another important part of the BSDP-program, a short overview is given below. The rest of this report will focus only on the geology and paleomagnetism of the rocks from the BSDP-program.

1.2 BSDP: Origin of life

Study on pillow basalts of the BGB has provided evidence for traces of 3.47 Ga old bacteria (Furnes *et al.*, 2004). These structures form during alteration of basaltic glass and are often called 'palagonite' (Thorseth *et al.*, 1992). Granular and tubular structures have been recognized in palagonite in many natural volcanic glasses in the margins of sea floor pillow basalts with different ages. It is suggested by several studies (e.g. Thorseth *et al.*, 1992; Furnes *et al.*, 2004) that microbial activity, by macro- and microorganisms that live within rocks (McLoughlin *et al.*, 2007), produces these structures during the process of extracting nutrients from the volcanic glass. These structures, when found in rock, are called trace fossils since they record the behaviour of organisms. The process of creating these biogenic structures is proposed by Thorseth *et al.* (1992). They suggest that the dissolution of the glass is started when colonizing microbes cause local variations in the environment on microscale by changing pH values. Since the solubility minimum of silicate glasses is near neutral pH, variations in the pH help the microbes to chemically drill into the substrate and create so-called pit-textures. These pit-textures result finally in granular and tubular textures (Thorseth *et al.*, 1992; Furnes *et al.*, 2001d). Recognizing those granular and tubular textures in basaltic rock is helpful in the search for the presence

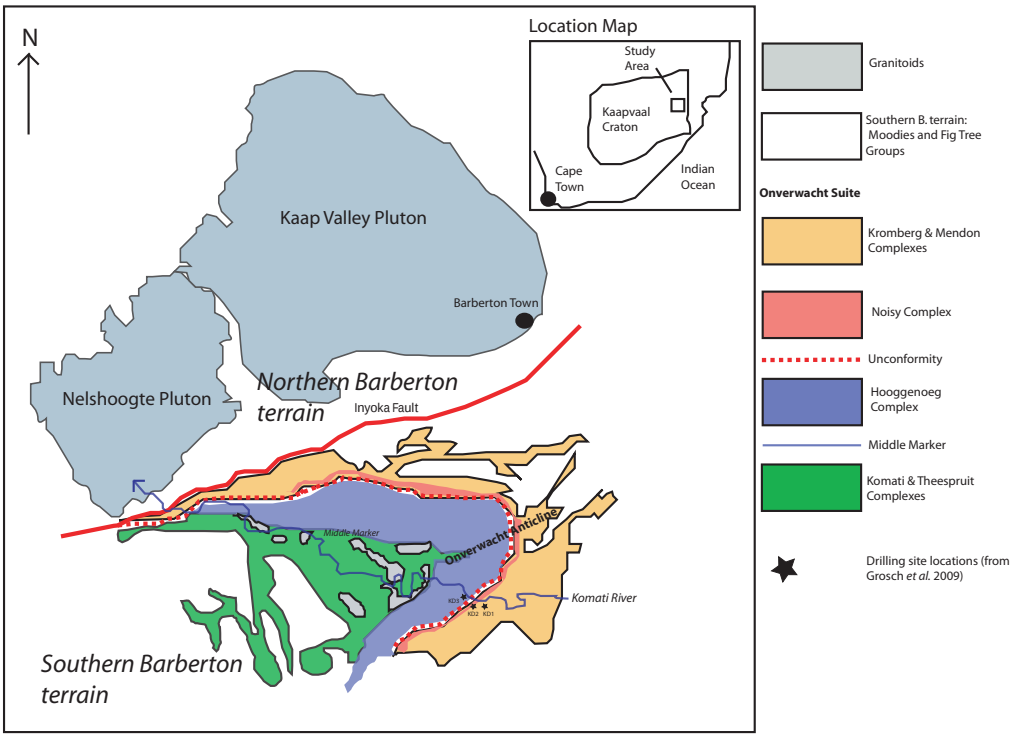

A

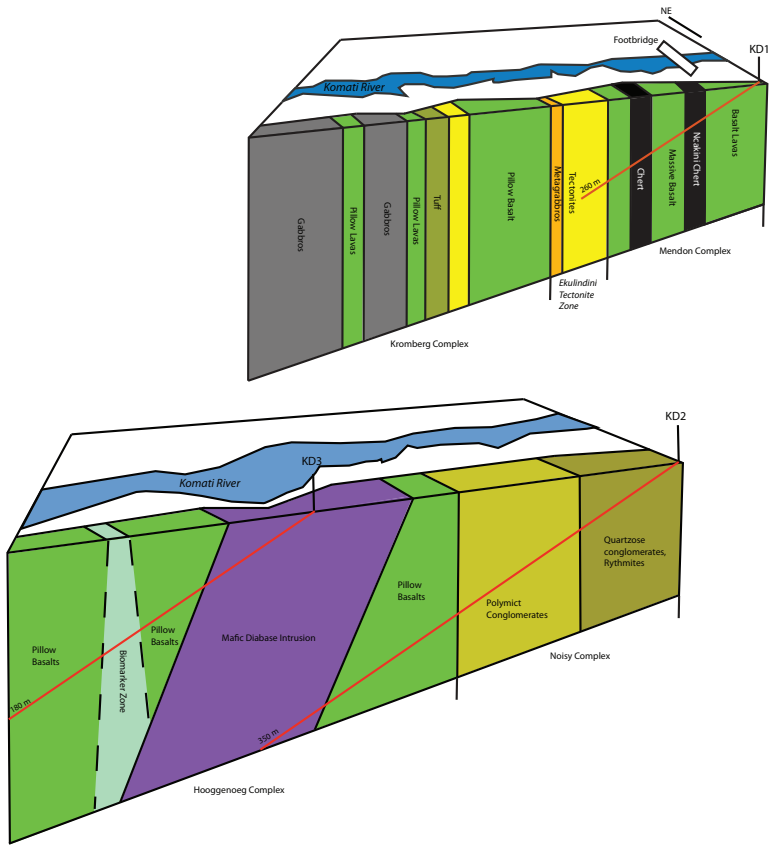

B (Simplified after Grosch *et al.* 2009)

FIGURE 1. A) Simplified geological map (based on de Vries et al. 2006 and de Wit, 2004) of the field area, with location map (upper right) showing geographical position. The large Kaap Valley and Nelshoogte plutons are indicated with a grey color. The red line at the eastern end of the studied area is the large Inyoka Fault, dividing the area in the Northern and Southern Barberton Terrains.The different complexes in the Southern Terrain are colored as follows: green – Komati Complex, Blue – Hooggenoeg Complex, Pink – Noisy Complex, Yellow – Kromberg Complex. The blue division between the Komati and Hooggenoeg Fm is the Middle Marker, indicated in several other studies. The light-grey areas inside the Komati Fm are granitoids. B) Simplified block diagram (after Grosch et al., 2009) with the different complexes and the positions of the three bore holes KD1 (position S26o02'15.3", E031o00'00.0", total depth: 261m), KD2 (position S26o01.500', E030o59.326', total depth: 350m) and KD3 position: S26o01'25.3", E030o59'16.6", total depth: 180m), all marked with a star in figure A.

of microbial life in that specific rock. Until recently, ages of biogenicity in rocks ranged from present (Furnes *et al.*, 2004) down to mid-Proterozoic (Furnes & Muehlenbachs, 2003). In situ trace fossils found in the pillow basalts of the BGB, outcropping at the banks of the Komati-river (Fliegel *et al.*, 2010), have been indicated by this method of Thorseth *et al.*, 1992. U-Pb dating of these trace fossils give an age of 3.34 Ga. This dating is better constrained than the dating of the traces of Furnes *et al.*, 2004; and is now taken as the oldest traces of life on Earth.

The drilled core from the BSDP-project provides a unique range of fresh, in situ rocks to find more evidence for the oldest trace-fossils ever found. A biomarker zone consisting of pillow basalts in the Hooggenoeg Complex, described and studied by Furnes *et al.* (2004), is included in the drilled rocks from the BSDP-project. This biomarker is present in the third core, KD3 (Figure 2). Researchers involved in the BSDP-program will study these pillow basalts which will provide information on the presence and diversity of early life under hydrothermal conditions in the Archean oceanic crust (Grosch *et al.*, 2009). Besides the search for early life on Earth this insight in trace fossils can be a next step in the search for life on extraterrestrial planets like, for example, Mars (McLoughlin *et al.*, 2007).

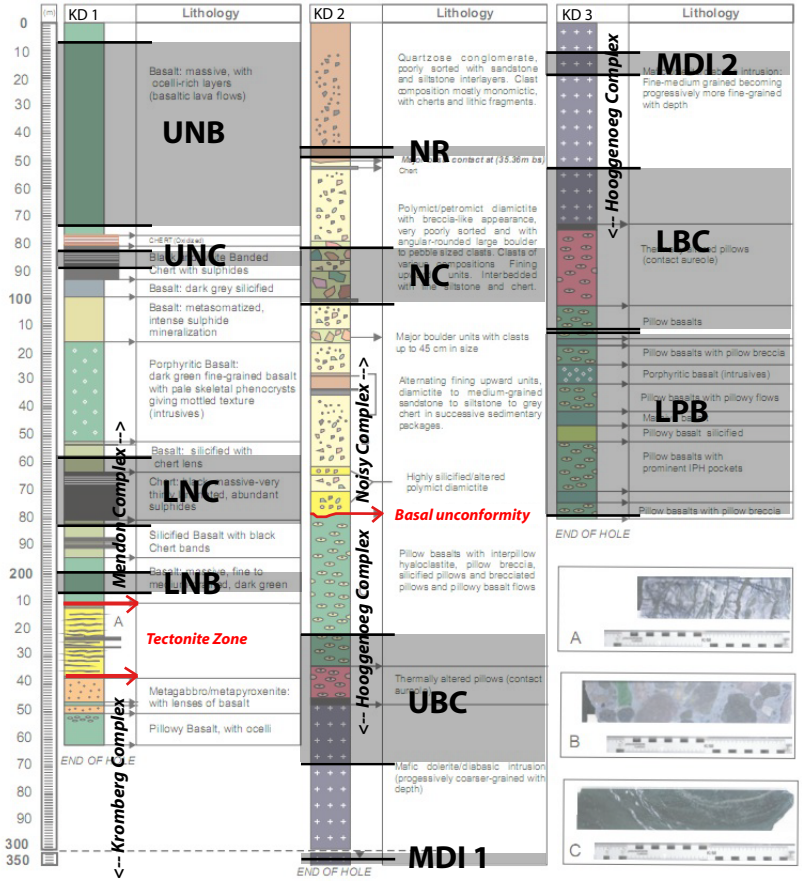

FIGURE 2. Site locations of this study indicated with grey boxes in stratigraphic order plotted over the stratigraphic column from Grosch et al. (2009). See Table 2 for an explanation of the codes.

2 BSDP: Geological Setting and stratigraphy

2.1 Geological overview

The Barberton Greenstone Belt, South Africa, is part of a NE-SW trending tectono-metamorphic belt and is located close to the eastern margin of the Kaapvaal craton (Figure 1A). The Kaapvaal craton, covering an area of about 1.2 x 10^6 km^2 , retains a substantial portion of rare mid-Archean rocks (3.0-4.0 Ga) (de Wit *et al.*, 1992). Equivalent rocks can only be found at two other places on Earth: 3.6-3.8 Ga old rocks in western Greenland (O'Nions & Pankhurst, 1978; Bennett *et al.*, 2002) and ~3.5 Ga rocks of the Pilbara craton in northwestern Australia (Tessalina *et al.*, 2010). The Kaapvaal craton is subdivided into a number of subdomains with the core of the craton consisting of at least three of these subdomains: the Ancient Gneiss terrain, the southern Barberton terrain and the northern Barberton terrain (see Figure 1A and de Wit *et al.*, 1992). The latter two form the BGB. A major fault zone, the Inyoka Fault, acts as the boundary between the southern and northern Barberton terrains. This fault is suggested to represent a tectono-stratigraphic boundary because of differences in stratigraphy, age and depositional environment between the rocks from both sides of the fault (Hofmann, 2005).

In the south of the southern Barberton terrain a dipping folded structure, the 'Onverwacht Anticline', is cross-cut by the Komati River, exposing fresh rocks of Archean age (Figure 1A). These rocks belong to the Swaziland Supergroup, often referred to as the Barberton Supergroup or Barberton Mountain Land (Hofmann, 2005; Ward, 1999; de Wit *et al.*, 2011), and several surface geology studies have examined these rocks (e.g. Usui *et al.*, 2009; Biggin *et al.*, 2011; de Wit *et al.* 2011, Furnes *et al.*, 2011). The terrain of the Barberton Mountain Land is subdivided in three main groups: the Onverwacht, Fig Tree and Moodies Groups. These units are tightly folded with large shear zones separating some of the folded structures (e.g. Hofmann, 2005; de Wit *et al.*, 2011). The large structure of the Onverwacht Anticline resulted from rotation of east-west trending isoclinal folds (Ward, 1999). The folding affects rock formations from the Onverwacht Suite. From young to old, these are: the Mendon & Kromberg Complexes, the Noisy Complex (in older literature this complex is the youngest part of the Hooggenoeg Complex), the Hooggenoeg Complex and the older Komati, Theespruit and Sandspruit Complexes (Ward, 1999; Grosch *et al.*, 2009). The Sandspruit Complex is not pronounced in the Onverwacht Anticline. Recent work showed that the stratigraphy of the Onverwacht Group is discontinuous, which led to the renaming of the different stratigraphic units: the Onverwacht Suite is formerly named as the Onverwacht Group and the former named formations of the Onverwacht Suite are now referred to as complexes (see de Wit *et al.*, 2011 for more detail).

2.2 Stratigraphy

The Mendon Complex (< 3334 Ma, Kröner *et al.*, 1996) is remarkable because of its large amount of chert lenses in between the basalts. Most cherts appear as very dark, black bands and show a thin lamination and are therefore easily to distinguish from the basalts. The part of the complex which is cored for the BSDP-project consists of massive basalt flows. These basalts are green in color, which is due to metasomatism and silicification. The drilling hole in the Mendon Complex (KD1, Figure 1B) ends with 10 m of pillowy basalt, stratigraphically situated beneath a Tectonite Zone which is described as a carbonated shear zone with chert lenses. This Tectonite Zone acts as the boundary between the Mendon Complex and the Kromberg Complex (Grosch *et al.*, 2009).

Both drilling holes KD2 and KD3; named KD2a and KD2b respectively in Grosch *et al.* (2009) (Figure 1B), include the Hooggenoeg Complex (ca. 3472 ± 5 Ma, Armstrong *et al.*, 2009). The most upper part of the Hooggenoeg Complex is now called the Noisy Complex (< 3470 Biggin *et al.,* 2011; de Wit *et al.*, 2011) which acts as a boundary between the Kromberg and the more mafic Hooggenoeg Complexes. The Noisy Complex is very different in lithology compared to the volcanic dominated other two complexes: it consists of conglomerates and sandstones interbedded with fine siltstones and cherts. A sequence of rhythmites is present in the top of the Complex (Grosch *et al.*, 2009).

In drilling hole KD2 a basal unconformity separates the Noisy from the Hooggenoeg Complex. The Hooggenoeg Complex has a cyclic nature of volcanism (Viljoen & Viljoen, 1969) characterized by pillow basalts and lava flows. This structure is intruded by a large mafic diabase intrusion, present in both KD2 and KD3, causing alteration of the pillow basalts in the contact aureole. The end of hole KD3 contains early Archean biomarkers or ichnofossils in a zone known as the 'Biomarker Cliff'(see Figure 1B and Grosch *et al.*, 2009; Furnes *et al.*, 2004) which is important for understanding the initiation of life on Earth.

3 Barberton Greenstone Belt

3.1 Deformation and metamorphic history

Through geological time many metamorphic and deformation events occur in different settings. Since the old age of Archean rocks, many events could have influenced these rocks causing for example mineral compositions to change, structures to develop and paleomagnetic signals to be overprinted. Therefore it is very important to know the geological history of the examined rock, especially when paleomagnetism is being used since original signals could be lost through time. When the geological history is better constrained, paleomagnetic data can be better interpreted.

All rocks in the BGB have been folded and faulted with general dips of vertical to sub vertical (Knaush & Lowe, 2003). The thick sequence of rock is explained by de Wit *et al.* (1982) as a repeated, 3-4 km thick section of folded and faulted rocks. This section is interpreted as an ophiolite representative of oceanic or back-arc basin crust, named the Jamestown Ophiolite Complex (de Wit *et al.*, 1987; de Wit, 2004). A significant feature of the metamorphism in greenstone belts is the absence of glaucophane (or blueschist) metamorphic facies (Viljoen & Viljoen, 1969). It is known that metamorphism in the BGB, as with most greenstone belts (Viljoen & Viljoen, 1969), is only low-grade metamorphism: in the igneous rocks the regional metamorphism never exceeds the greenschist-facies to low-amphibolite facies (de Wit *et al.*, 1987). However, rocks from the Onverwacht Suite from the BGB were never exposed to temperatures above 400°C (Biggin *et al.*, 2011; Furnes *et al.*, 2011). Studies on peak metamorphic conditions of parts of the Komati and Hooggenoeg Complexes indicate that these conditions existed immediately after the formation and burial on the seafloor (Schoene *et al.*, 2008). The earliest period of the BGB holds the most complete geological evolution, followed by a period of ~3 Gyr of relative stability (Schoene *et al.*, 2008). A short summary of the most important events is given here with a focus on events relevant for the paleomagnetic signal in the BGB rocks.

3.2 Important events

Dating of zircons by Kamo & Davis (1994) has given reliable age constraints for most geological events in the BGB. At least 4 deformation phases (D1-D4) have been recognized in the BGB (de Vries *et al.*, 2006). Deformation phases D1 (3445 Ma) and D2 (3232 Ma) represent a period of maximum 15 Myr of major compression deformation and shortening in the BGB resulting in folding and thrusting of the geological units (Kamo & Davis, 1994; de Vries *et al.*, 2004). Synchronously to this compression event, sedimentation of clasts occurred forming the Noisy Complex (Usui *et al.*, 2009). Further folding and faulting during D3 (ca. 3227 + 4/-3 Ma, Kamo & Davis, 1994) resulted in large-scale structures like the Onverwacht Anticline. This event included sedimentation and thrusting of at least the upper Fig Tree Group and much older slivers of rock and took place probably coeval with the emplacement of the Kaapvaal pluton. A lot of upright, near-vertical folds have been recognized through the BGB (for example Ward, 1999; de Wit *et al.*, 1987). These folds have been formed during D4, the last major geological event. The minimum age for this event is 3216 +2/-1 Ma (age from the Dalmein Pluton, Kamo & Davis, 1994) which is the same age for the deposition of supra crustal rocks in the BGB which are all affected by the folding. Zircon dating of the Mudpools porphyry, which cross-cuts the folded sediments of the Fig Tree Group (de Ronde *et al.*, 1991), gives an age of 3227 ± 1 Ma. This age is therefore the maximum age for D4 and places this event coeval with the emplacement of the Kaapvaal craton as well (de Ronde *et al.*, 1991). After these events the rest of geological time was relatively quiet at the regional scale of

Overprint Component	Removal T (°C)	declination (°)	inclination (°)	α95 (°)	Polelat (°)	Polelong (°)	α95 (°)
LT1	250	350.7	-60.6	9.6	72.6	234.9	12
LT2	100 - 440	162.8	-66	14.3	-13.6	199.5	22.2
MT	370-480	321.8	85.6	13.1	-18.6	32.6	33.6
Reference value							
GAD		0	44.3				
Karoo		330	-53				
PDF		342	-63				
Bushveld Complex					19.2	30.8	5.8

TABLE 1. Overview of overprint components from Biggin et al. (2011) with their reference values. Declination, inclination and Paleolatitude, Paleolongitud are given, both sets with error values.

the BGB. One larger scale event, however, could be of great influence on the paleomagnetic data from the BGB as indicated by the results of surface rocks from the Onverwacht Group by Biggin *et al.* (2011): the Karoo large igneous basalt province at ~180 Ma. This event was a major Mesozoic remagnetization and is believed to have remagnetized 7 sites (clustered as 'HT1') from the study of Biggin *et al.* (2011). Other large scale events which could possibly have affected the magnetic signal in the BGB rocks are: the intrusion of the Bushveld Complex at ~2.057 Ga, the Vredefort Meteorite Impact at ~2.017 Ga, the Waterberg Large Igneous Province at ~1.87-1.98 Ga and the Natal-Namaqua orogenic event at ~1.040 Ga (cf. Strik *et al.*, 2007). From these events only the Bushveld intrusion is found as a second possible overprint signal ('LT2') in the surface rocks from Biggin *et al.* (2011). See Table 1 for an overview of the expected overprint signals for this study.

4 Methods and Background

4.1 Sampling

In the period July-August 2008 the first phase of scientific drilling inside the BGB was completed by the AEON (African Earth Observatory Network)-BSDP team. From the three drilling holes, in total 800 m of core with 99.9% recovery was brought to the surface. Drilling directions for hole KD1 ('KD' stands for 'Kromdraai' which is the translation for Elukideni, a town nearby the drilling sites) and KD2 are towards 317° (NW) with a drilling angle of 45°. The third hole KD3 had a drilling direction towards 337° with an angle of 43° (see Grosch *et al.*, 2009 for exact locations of the drilling sites). These shallow-dip drilling directions were needed to get drilling holes with an orientation perpendicular to the bedding of the geological units. To orientate the cores a core orientation tool, 'Easymarker', was used during drilling (Grosch *et al.*, 2009). This tool marked the core pieces with a gravity line at the bottom of the core, so the different parts (all of approximately 3 m) could be fitted together at the surface; the gravity line was traced with a blue line. Once brought to the surface the cores were washed with clean water and two other orientation lines where put on the cores in a core shed. A red line at 180° from the blue line was marked as the top of the core and a black line was marked in between the blue and red line. Arrows put on the cores indicate the top of the drilling hole which were put on before logging and cutting the cores in half along the black line. A diamond blade core cutter was used for the cutting. After this the top part of the cores where packed in wooden boxes and shipped to Norway for the University of Bergen and the bottom parts were packed in other wooden boxes and stayed in South Africa at Cape Town University.

In August 2010 our paleomagnetic team sampled the BSDP-cores in a rock-storage at Cape Town University. Samples were drilled with a special custom made drill-bit on an electrically powered hand-drill, perpendicular to the blue line on the cores. Small cores with 12 mm diameter and a length of ~ 20-25 mm were sampled through the whole cored section. The same diamond blade core cutter as used at the drilling site was used as work-bench for the

FIGURE 3. Impression of sampling the drilling cores in Cape Town. A) The wooden boxes in which the cores (already cutted in half) were transported and stored. B) Vertical drilling of a core-piece on the wooden construction on the saw-table. At the right-top of the photo the saw is visible. C) Example of a small core sample. D) Part of a core after drilling of samples for this study.

vertical drilling (see Figure 3 for sampling setting). Testing with a magnetic compass resulted in the discovery of a large magnetic field originating from the table-construction of the core cutter. A wooden construction was made to act as a standard fixed on the table-construction with minimum influence from this magnetic field. Since the cores were cut in half at the drilling side, lying in a gutter perpendicular to the saw, the magnetic field of the table likely influenced the magnetic signals in the cores already at the drill location. This would result in an overprint of the paleomagnetic signal with a direction towards the cutting direction. In principle, cutting was accomplished along the black marking line, which direction is coeval with the drilling directions of the cores: 317/45 for KD1 and KD2 and 337/43 for KD3. An overprint due to the cutting is expected to give directions comparable with the drilling directions of the drilling holes. This has major implications for the interpretation of the paleomagnetic data. If this overprint is present, extra sample handling is needed before demagnetization of the samples, which is described below.

In total 508 samples were collected: 87 from sites in the Mendon Complex, 68 in the Noisy Complex and 353 from sites in the Hooggenoeg Complex. Paleomagnetic sampling sites (Figure 3 and Table 2) have been selected by the characteristics of the three complexs to get a good overview of the different paleomagnetic properties of lithologies throughout the Onverwacht Suite. Extra orientation measurements and corrections were needed since not all cores were orientated accurately at the drilling location: in many cases imprecise cutting along the blue line resulted in a deviation of several degrees for our vertical drilling. In some cases, the top-part of the core instead of the bottom-part was sent to Cape Town University. Detailed and accurate logging of these deviations made it possible to construct corrections

for these orientations. These time-consuming corrections are crucial, however, since the orientation of the sampled cores influences the output of paleomagnetic measurements.

4.2 Measurements

4.2.1 Verwey transition

The collected samples were taken to the paleomagnetic laboratory 'Fort Hoofddijk' at Utrecht University for the paleomagnetic measurements. Selected samples for demagnetization were first cut to cores of all the same size with a volume of ~2 cm^3. The remaining samples were stored for other measurements. Eight samples selected through the different sites were cut in half in an A and B side, to test the best method to get rid of the suspected overprint from the cutting-table. A-sides were put in liquid N_2 in a shielded room for several minutes, after measurement of the natural remanent magnetization (NRM) using a horizontal 2G SQUID cryogenic magnetometer (noise level $3x10^{-12}$ Am^2). This cooling gets the samples through the 'Verwey transition': the multi-domain (MD) component would be mostly removed while a single-domain (SD) or pseudo single-domain (PSD) component is hardly affected (see Walz, 2002 for a complete review on the Verwey transition). Since MD grains are energetically more favorable to form magnetic domains, an overprint signal would be in most part accommodated in the MD component. We expect therefore that after the N_2-treatment most of the overprint signal is removed in the samples. Demagnetization would then remove the original NRM of the samples. The B-sides of the test samples were demagnetized with alternating field using the in-house made 'robot': a 2G magnetometer with an inline alternating field (AF) demagnetizer attached to an automatic sample handler. Demagnetization steps of 0,2,4,6 and 8 mT were used as a test to compare the result with the N_2-method.

Code	Name	Hole	Complex/Fm	n	iNRM (mA/m)
UNB	Upper Ncakini Basalt	KD1	Kromberg	9	0.075
					75
UNC	Upper Ncakini Chert	KD1	Kromberg	2	0.365
					0.9
LNC	Lower Ncakini Chert	KD1	Kromberg	5	0.5
					6
NR	Noisy Rhythmites	KD2	Noisy	4	0.035
					0.475
NC	Noisy Conglomerates	KD2	Noisy	9	0.0375
					0.713
UBC	Upper Baked Contact	KD2	Hooggenoeg	44	0.18
					16000
MDI	Middle Diabase Intrusion	KD2+3	Hooggenoeg	15	1000
					3000
LBC	Lower Baked Contact	KD3	Hooggenoeg	38	16.5
					9000
LPB	Lower Pillow Basalt	KD3	Hooggenoeg	31	0.55
					17000

TABLE 2. Names of the drilled sites with their representing codes. For each site an overview of number of samples per site and their initial intensity values (iNRM) is given. First value is minimum value found in the site, second value maximum

4.2.2 Thermal (TH) demagnetization

Thermal demagnetization on the 2G cryogenic magnetometer was performed on a total of 2x80 samples. The first run of 80 samples was selected through the whole section, with 62 samples treated with N_2. All these 80 samples were measured stepwise with increments of 30°C up to a temperature of 420°C. After this heating step some

samples were rejected for further measurement because of low intensities. The rest of the samples were measured up to 590°C with increments of 50°C to 10°C at the highest temperatures. Demagnetization diagrams showed a drop in intensity after the N_2-treatment, but unfortunately, no clear overprint-component was completely removed. Therefore it was decided that the next 80 samples would not be treated with N_2. Larger temperature steps were used for the low temperature demagnetization: 50-80°C up to a temperature of 450°C. Increments of 30-10°C were used to remove the remaining NRM from 480-500°C onwards.

The second run of 80 samples was selected throughout the Hooggenoeg Complex to perform a baked contact test around the mafic diabase intrusion. When a rock is heated, ferromagnetic minerals are free to rearrange to the magnetic field during the time of heating; it acquires a new thermoremanent magnetization (TRM). The baked country rock and the igneous inrusion therefore acquire the same TRM. When the characteristic remanent magnetizaion (ChRM) direction of the baked country rock and the igneous rock are similar, it provides an indication that the ChRM direction is stable and may represent a primary NRM. This baked contact test was performed on the rocks of the Hooggenoeg Complex. The test is passed when a gradual change in ChRM directions of the unbaked country rock and intrusion is found. This is to be expected when the age of the country rock is significantly older than the age of intrusion. However, uniform ChRM directions for all three rock-types (unbaked country rock, baked country rock and igneous rock) indicate a remagnetization for all lithologies, and the baked contact test is failed (Butler, 1992). This remagnetization event must then have occurred after the intrusion of the igneous rock and cooling of the baked contact.

4.2.3 Alternating Field (AF) demagnetization

To support the thermal demagnetization data, four runs of each 12 samples on the in-house built robotized sample handler controller, attached to a horizontal 2G Enterprises DC SQUID cryogenic magnetometer, named the 'robot', were performed. All runs were first stepwise demagnetized up to 10 mT with increments of 2 mT to try and remove the overprint signal. The first run holds the A and B-sides of eight samples tested for N_2 and AF treatment plus four extra samples. Demagnetization was performed with steps of 3-10 mT from 10-100 mT. The same scheme was used for the second and third run which holds samples of low intensities and samples from the baked contact respectively.

A gyroremantent magnetization (GRM) was acquired in many samples from the first three AF-runs. This GRM is described by Dankers & Zijderveld (1981) as "the occurrence of an increase in remanence when the alternating field is high, named as 'disturbing magnetizations'". The nature of the disturbance is explained in two ways. Dankers (1978) suggest that the disturbance is probably caused by the rotation of the unblocked magnetic moments of anisotropic grains. The rotation is directed from the alternating magnetic field direction to a direction of easy magnetization of the grain, during reduction of the alternating field to zero. These disturbing magnetizations occur if the directions of easy magnetization in the rock are not symmetrical around the direction of the alternating field. On the other hand, Stephenson (1980) states that the disturbance can be introduced by a direct equivalent magnetic field of gyromagnetic origin, which is caused by the relaxation of unblocked, magnetic moments. The relaxation is from the alternating field direction towards the easy magnetic direction, and orientated perpendicular to the alternating field. This GRM is most pronounced when greigite is present as magnetic carrier in the rock, and is produced in any specimen with constituent magnetic particles which are non-

randomly orientated and which are of the appropriate size and composition. A method constructed by Dankers & Zijderveld (1981) compensates the effect of disturbing magnetizations. From a theoretical basis described by Stephenson (1993) it follows that these disturbing magnetizations can be named as GRM when this Dankers & Zijderveld-method (or DZ-method) works. Theoretically this is described as method 2 in Stephenson (1993). In short this method can be outlined as follow:

- For each AF-step a sample is demagnetized as usual with consecutively the X, Y and Z axis parallel to the coil axis.
- The specimen is then subsequently demagnetized for a second time at the same peak field but now with the X-axis parallel to the coil axis, and the total remanent magnetization is measured. This step is repeated with respectively the Y and Z parallel to the coil axis.
- Now, for each demagnetization step, three times three components of remanence exist, which can be combined to give the corrected component:

		Components of remanance remaining		
AF applied	X	*M1x*	M1y	M1z
along	Y	M2x	*M2y*	M2z
	Z	M3x	M3y	*M3z*

From the overview above, the corrected component $\mathbf{M} = \mathbf{i}\, M_1x + \mathbf{j}\, M_2y + \mathbf{k}\, M_3z$.

It is important to use this DZ-method for samples which are prone to acquiring a GRM during stationary AF demagnetization. In our laboratory we call this method the 'per component' or 'pc' method and it was applied to the samples of the fourth run. Demagnetization on this run was performed up to 85 mT with steps of 3-15 mT (from 10 mT on).

4.2.4 Magnetic carriers

Curie-balance measurements and decay-curves of demagnetized samples provide insight in the most important magnetic carriers and give important information about the different components present. This can be used to choose the best demagnetization steps for isolating the ChRM. Decay curves were constructed for all measured samples through the whole section. Curie-balance analyses were performed on 11 samples through the baked contact of the Hooggenoeg Complex and on one low-intensity sample from the Noisy Complex. The main magnetic carriers in magnetic rocks have different Curie temperatures: 578°C for magnetite, 640°C for maghemite and 680°C for hematite (Dankers, 1978; de Boer, 1999). When (titano) magnetites are present in a rock the Curie temperature decreases to a value near 500°C. This is found mostly in basalts and can be expected in the rocks of this study (Dunlop, 1982).

Assessing the presence of maghemite in a rock is important for paleomagnetism: low temperature maghematization is a process which oxidizes the (titano) magnetites without disturbing their crystal lattice, at temperatures lower than 250°. They are metastable at room temperature, and they will invert tot (titano) hematite when they are heated to temperatures above 350°C. Since maghemite is instable above temperatures of 350°C the Curie point cannot be measured exactly, but is likely around 640°C (Heider & Dunlop, 1987). When a drop in intensity in the Curie diagram near 350°C is recognized, maghemite can be present as one of the magnetic carriers. This holds only for small-grained (15 - < 5 μm) samples (de Boer, 1999).

4.2.5 Conglomerate test

From the Noisy Complex, 51 samples were measured from 20 different conglomerate clasts to perform a conglomerate test. The main objective of this

conglomerate test is to use the distribution of magnetization directions from different clasts to show if the found remanence is likely to be primary or not. Since clasts are randomly distributed in a conglomerate rock, the magnetization directions of the clasts are expected to be found randomly as well. This holds only if no remagnetization event has occurred after the deposition and lithification of the conglomerate rock. An important factor in this test is the time between the formation of the host rock and the formation of the clasts in the conglomerate rock. When this time-lap is relatively small, the found remanence is more likely to be primary (Shipunov *et al.*, 1998).

In the conglomerate test described by Shipunov *et al.*(1998) a null hypothesis H_0 ('a uniform distribution is present') is tested against an alternative hypothesis H_1 ('a preferred direction is present'). With use of a statistical procedure (see Shipunov *et al.*, 1998 for detailed information) a calculated ρ-value is compared with a critical value ρ_0. H_0 is either accepted ($\rho < \rho_0$) or rejected ($\rho > \rho_0$). When a secondary remanence can be isolated from the clasts this can be used as the reference direction, otherwise the secondary remanence of the host rock or directly overlying rock must be known (intra-formational conglomerate test). When these secondary remanences are not known precisely, this test is still accurate, since a deviation of less than 20° reduces the accuracy with only a few percent. This makes this 'Shipunov-test' more robust than other tests, for example the 'Watson-test' from Watson and Beran (1967).

Tests on surface rocks from the Noisy conglomerate were performed by Biggin *et al.* (2011). For the test on the BSDP-samples, reference values from the present-day field (PDF) and the Karoo overprint as in Biggin *et al.* (2011) were used since no secondary NRM of the host rock is available. Additionally, from the demagnetization diagrams of the conglomerate clasts, a third reference value was found by determining the secondary component and as a fourth reference value we used the geocentric axial dipole (GAD) field at the present latitude of the site.

4.3 Interpretation of demagnetization behaviour

Demagnetization diagrams were interpreted with the use of Zijderveld diagrams (Zijderveld, 1967). When no clear component could be determined, we interpreted the demagnetization data through great-circle analysis (McFadden & McElhinny, 1988). This method can be used to examine if a combined best-fit great circle can be plotted through the selected paleomagnetic directions. This can be used for example to determine if a found component correlates with the cutting-table direction. One other example of the use of the great-circle analysis when a high temperature (HT) component is largely overprinted. By the use of the great circle analysis, the expected direction of this HT-component can be calculated.

Statistics on the output-data can be performed by using a 45°-cut-off, which is usual in secular variation studies (e.g. Johnson et al., 2008). Data cut-off by this method can be excluded from further interpretation.

	Step	declination		inclination		intensity (mA/m)		error	
		AF	N2+AF	AF	N2+AF	AF	N2+AF	AF	N2+AF
LNB05	20	150.6	293.3	14	44.3	149.1	69	2	3.8
	19		229.5		61.6		57.7		4.1
	0	154.7	221.1	15	58.7	102.4	57.3	1	1
	2	155.9	218.2	16.1	58.8	71.7	50.3	1	1
	4	161.6	232.2	19.5	49.8	40.5	38.6	1	1
	6	217.6	237	-54.7	49.6	16.7	35.3	1	1
	8	276.2	248.5	-12.2	54.9	9.5	26.2	1	1
	21	276.6	253.1	-11.4	52.3	8	26	2.8	3.3
UBC40	20	102	117.9	-29.7	-26.4	170.5	323.8	98.9	67
	19		65.1		-29.8		409.5		34.8
	0	106.3	97.5	-31.7	-45.8	2000	2000	1	1
	2	106.1	97.4	-34	-46.5	2000	2000	1	1
	4	105.3	97.5	-37.7	-47.1	2000	2000	1	1
	6	104.2	97.4	-40.3	-47.7	2000	2000	1	1
	8	103.3	97.2	-42.3	-48.3	2000	2000	1	1
	21	103.4	49.4	-44.1	-27.3	2000	372.9	3.9	35.3
UBC74	20	201.6	292.9	53.7	48.8	108.6	401.1	223.8	63
	19		259.7		14.1		368.2		56.2
	0	320.5	279	49.5	19	9000	1000	1	1
	2	320.2	278.9	49.4	18.4	9000	1000	1	1
	4	318.8	278.8	49.2	18.3	8000	1000	1	1
	6	317	278.7	49.1	19.1	7000	1000	1	1
	8	314.7	278.5	49.1	18.1	5000	1000	1	1
	21	315.4	251.2	46.5	10	5000	253.2	4.5	98.5
LBC76	20	332.9	330.6	32.3	26.5	70.4	81.1	4.1	4.4
	19		337.2		11		49.7		3.7
	0	351.2	337.7	36.8	12.6	106.3	49.5	1	1
	2	347.6	336.1	30.3	8.8	100	49.8	1	1
	4	347.6	336.7	24.2	8	94.3	49	1	1
	6	350	336.6	21	8.1	85.1	48.7	1	1
	8	352.2	338.6	19.3	6.4	75.8	47.9	1	1
	21	350.7	339.9	20.8	12.2	78.7	49.8	3.2	3.6

TABLE 3. AF- and N2-method overview for four samples, cut in half. 20-step refers to TH-measurement at room temperature, 19-step refers to TH-measurement after N2-procedure and 20-step to TH-measurement after AF-procedure (for which 0-8 steps indicate the small mT-steps). Intensities in mA/m. Note the high errors for the 20-step for samples UGC 40 and UBC 74 due to use of wrong range on the cryogenic.

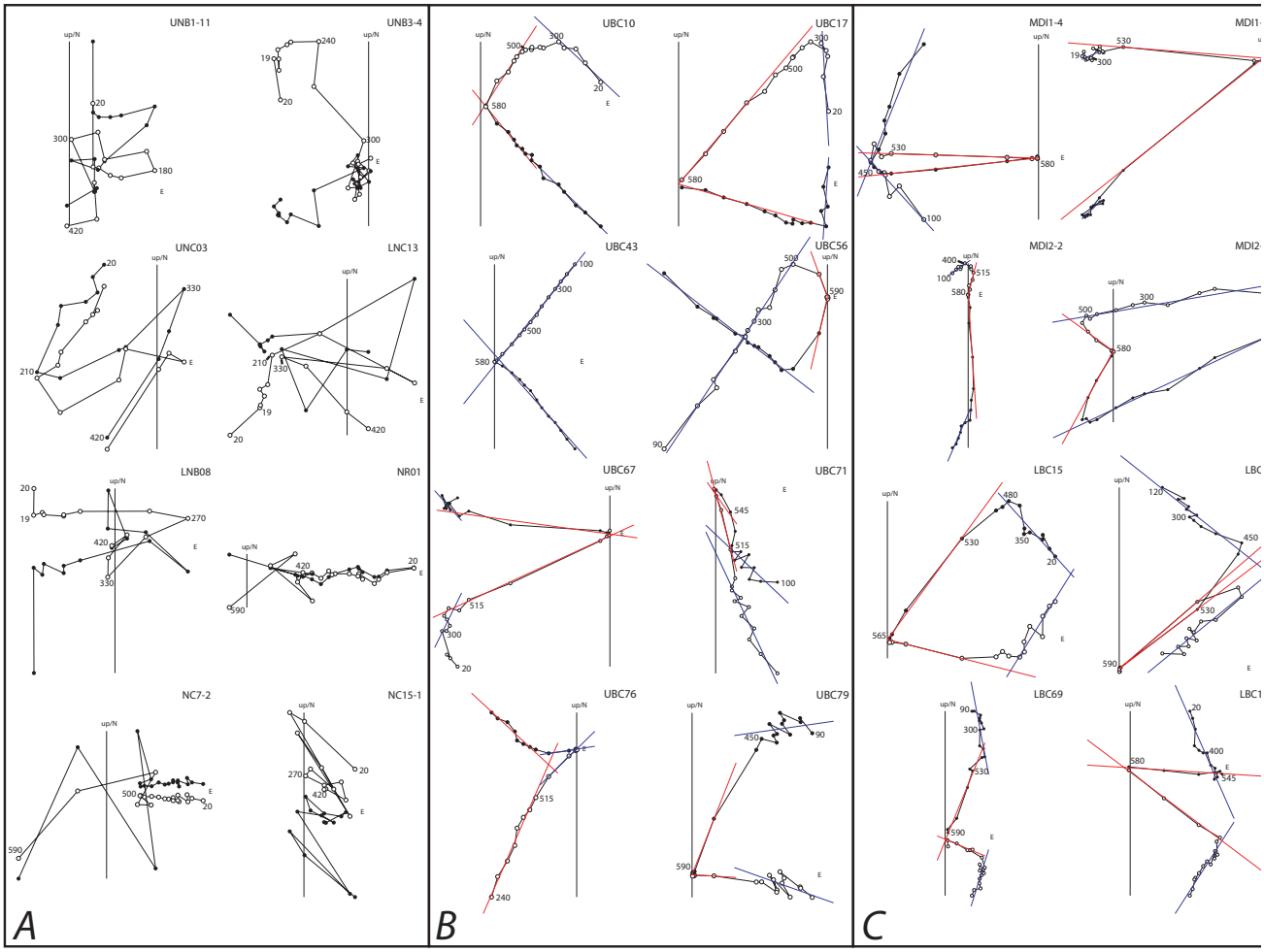

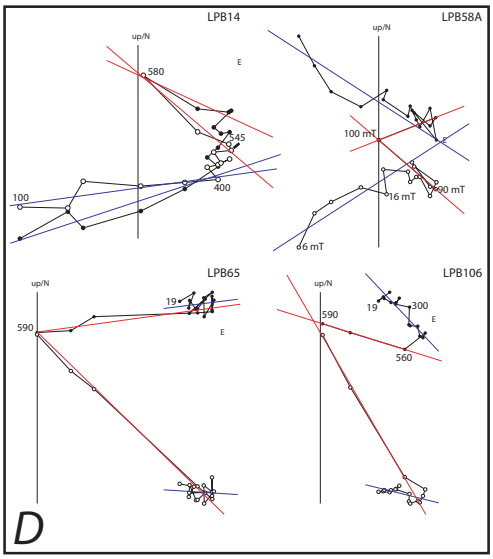

FIGURE 4. Examples of TH-demagnetization diagrams (Zijderveld plots) of samples from the different complexes: A) Kromberg and Noisy Complexes; B-C) Hooggenoeg Complex. Values in the diagrams refer to temperature steps. Blue lines show interpretation of the overprint direction, red lines interpretation of the high temperature (HT) component. Open symbols represent the vertical components. All diagrams are presented up/N.

5 Results and Interpretation

5.1 Overprint and ChRM components

Initial NRM intensities vary considerably through the whole section from 35 µA/m to 17 A/m (Table 2). Compared to the NRM intensities of Biggin *et al.* (2011) the values from this study are very high. Table 3 shows the intensity decay for both the N_2- and AF-method of four samples which have been cut in half in an A and B part and were treated for both methods. Unfortunately, errors are very high for the NRM-measurements for two samples (UBC 40 & UBC 74, see Table 3), giving unreliable data to compare these samples with the others.

After cooling with liquid N_2, a large drop in intensities is found and after a supplementary AF-treatment even a larger drop in intensity is visible. Samples which have undergone only the AF-treatment show in most cases a drop in intensity as well, but less compared to the combined method. Final declination

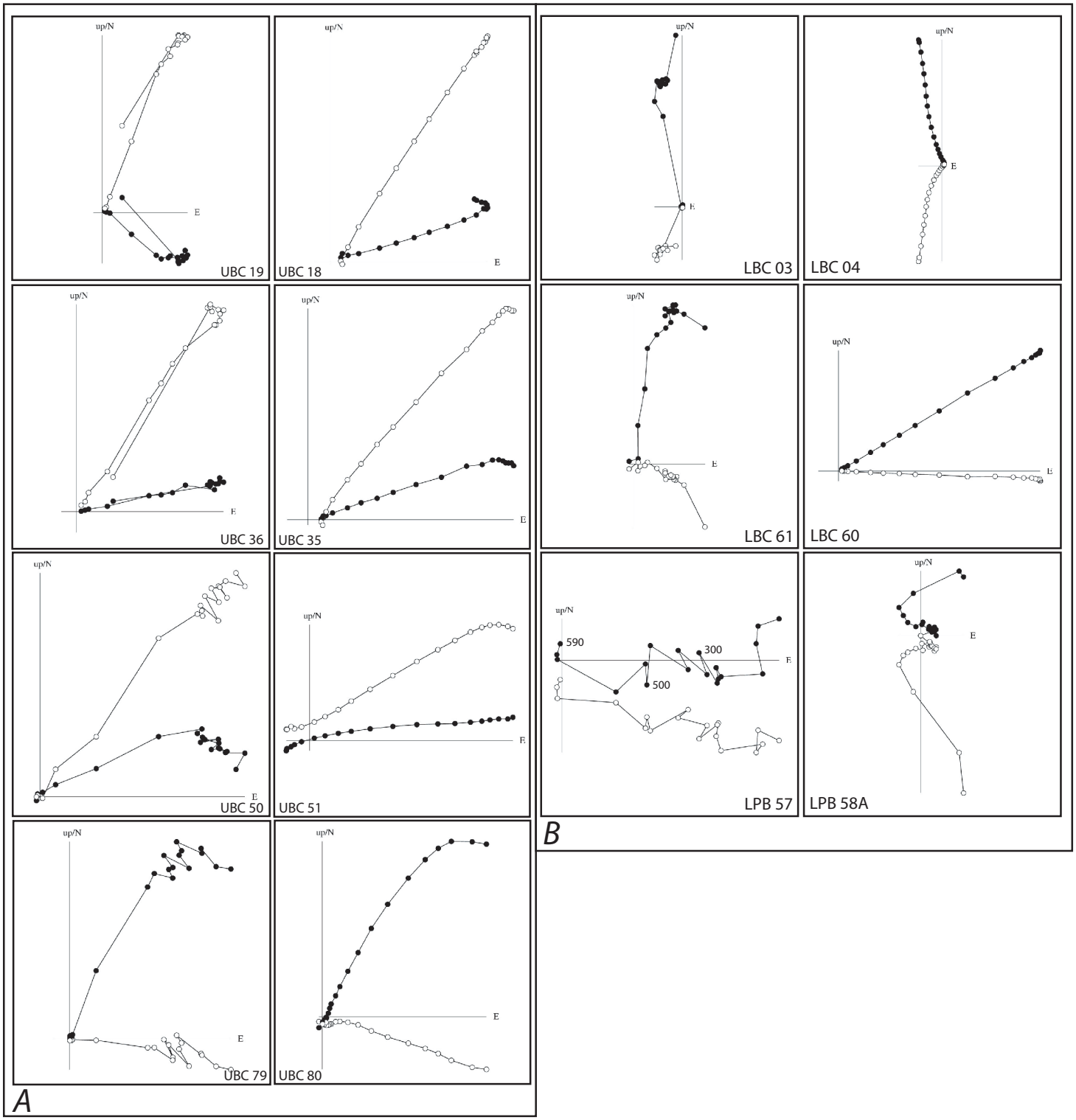

FIGURE 5. Demagnetization diagrams samples of the Hooggenoeg Complex (A) UBC; B) LBC and LPB). In every row the left sample represents TH-demagnetization and the right sample AF-demagnetization, with both samples from a positional very close. Steps are indicated in °C for TH-demag. and in mT for AF-demag. Most diagrams are similar. The TH-diagrams are pointing better to the origin and show more clearly the breakdown of the overprint component due to the N2-method. AF-diagrams show in most cases a cluster of dots for the breakdown of this component.

and inclination data differ for both methods which indicates that the overprint signal has not been destroyed completely. This is supported by the demagnetization diagrams: the overprint component can be recognized for most samples up to heating to at least ~300°C (Figure 4) but often up to 500°C or even higher; it will therefore be called the ‘ low temperature’ (LT) component. Often, a high temperature (HT) component can only be determined at temperatures higher than 480-500°C to ~580°C, with an overlap from the LT- to the HT-component from 300 to 500°C. Several demagnetization diagrams exclude

a clear division between the LT and HT component, making it difficult to determine any reliable component.

The results of AF-demagnetization compare well with those of TH-demagnetization of similar samples through whole the section (Figure 5). The HC-component in the AF-diagrams is in most samples removed from 25-30 mT up to 50 mT, at higher fields a GRM is often introduced (Figure 6). Figure 5 shows examples of near stratigraphical samples, one TH-demagnetized and the other with AF. One big difference between the two types of demagnetization is the removal of the overprint by the N_2+TH method *vs*. the low field AF method: in the TH-diagrams a big jump between the steps before and after the N_2-procedure is visible while this is expressed in the AF-diagrams as a small cluster. This is clear, for example, in the diagrams of UBC 19/UBC 18 and UBC 36/UBC 35 (Figure 5A).

Furthermore, a clear introduction of a GRM is recognized in most AF-demagnetized samples. The diagrams of samples UBC 51, UBC 80 and LBC 04 show a clear deviation of the demagnetization diagram from 50 mT on as an effect of the introduction of the GRM. As described in section 4.2.3, this disturbing magnetization needs to be compensated in order to interpret the diagrams in a right way. This is done with the pc-method for three samples (Figure 6), on which the standard (st) procedure is applied as well to make a good comparison. The top row of Figure 6 shows the diagrams using the st-procedure; the bottom row shows the diagrams using the pc-procedure. Only LPB 66 does not show an improvement in the signal after the pc-procedure, for the other two samples it appears that the pc-procedure is the best

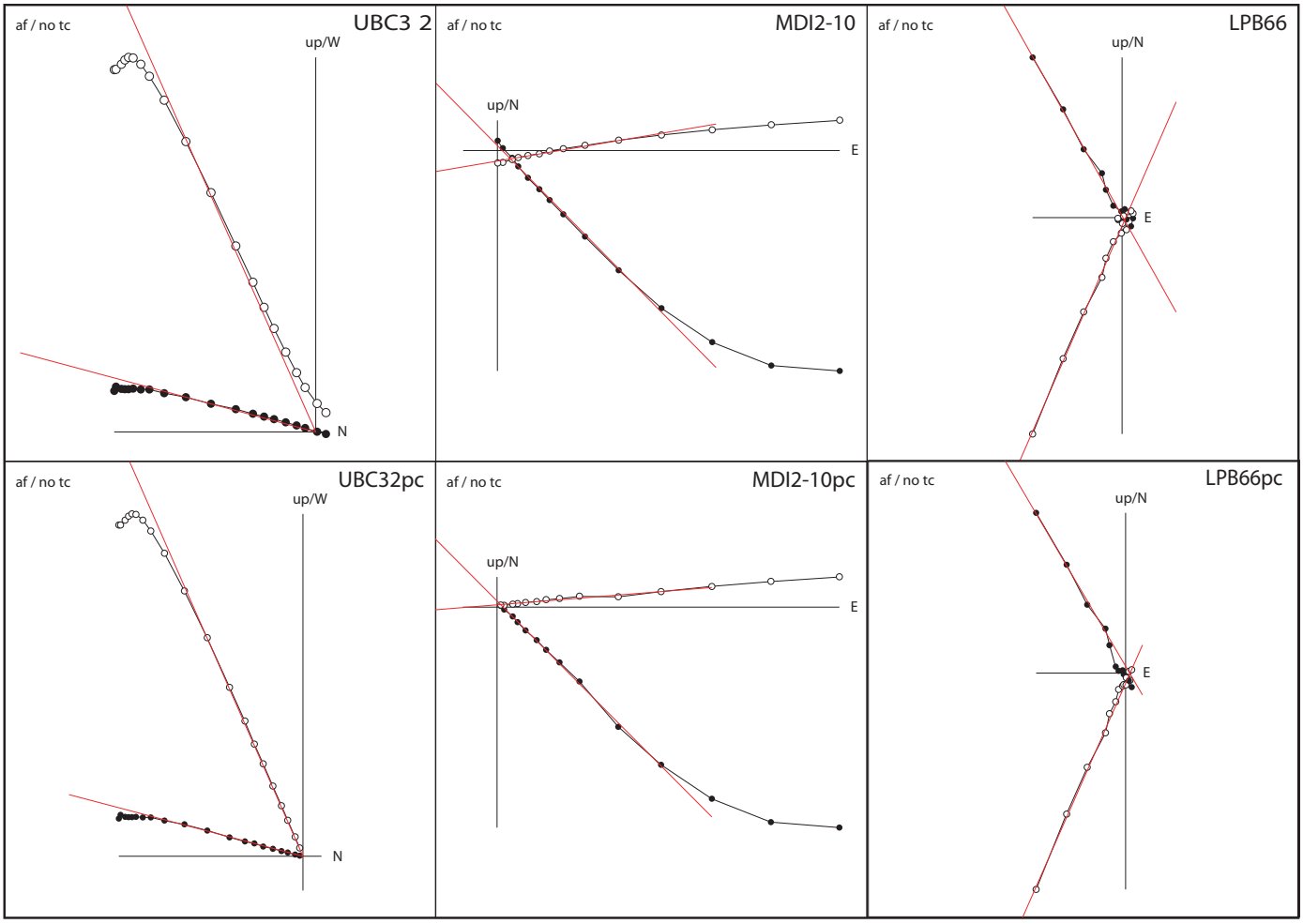

FIGURE 6. Three examples for AF-demagnetized samples with the standard (st) procedure (top row), and the per component (pc) procedure (bottom row). For sample UBC 32 it is very clear to recognize the deviation from the original direction due to GRM in the st-diagram, which is solved in the pc-diagram. For sample LPB 66 the pc-procedure does not fix the deviation and does not provide a better interpretation.

one for these kinds of samples. After this test, the pc procedure was therefore routinely applied.

The LT and HT components from the Mendon and Noisy Complexes (sites UNB, UNC, LNC, LNB, NR and NC) are very scattered and do not produce a reliable mean direction (Figure 4A). The number of measured samples is too low for some sites to use the great circle method on these samples in order to get an indication of the mean direction of these sites. The two components are well developed in most samples from the Hooggenoeg Complex (Figures 4B-D) and the number of demagnetized samples is high enough for the interpretation of mean directions. Our focus will therefore be mainly on the Hooggenoeg Complex in the following sections.

A selection of samples which will be used for interpretation of the data is needed, in order to create a reliable set of data with the best possibility to represent a (near) primary signal of the rocks. A step-wise selection is introduced here. The first step of the selection makes a distinction between samples with a clear two-component (LT and HT) diagram and samples that are too scattered. The results for the four remaining sites in the Hooggenoeg Complex (UBC, MDI 1+2, LBC, LPB) are shortly described below. In general it is found that the overprint in these samples is removed at temperatures of 420-500 °C for the TH method while a field of 10-30 mT is only needed for the AF method.

UBC (Figure 4B, 5 and 6): 32 out of 44 TH demagnetized samples show a clear difference between the LT and HT component. The HT component is mostly defined at temperatures higher than 500°C and occasionally at temperatures higher than 450-480°C. 16 samples were demagnetized with alternating field (AF). A GRM is recognized in most samples; this GRM is corrected with the pc-procedure for 5 samples. For 12 out of 16 AF samples two components are found, with the second component removed in most cases above 30 mT. In total 44 out of 60 measured samples can be interpreted as two component signals.

MDI (1+2) (Figure 4C and 6): 15 samples were TH demagnetized from which only one is excluded from the HT-component interpretations. The HT-component is recognized in most samples from 500°C up to higher temperatures. 2 samples, one of each MDI site, were AF-demagnetized (pc-method) with a high coercive (HC) component from 25 mT up to 70 mT.

LBC (Figure 4D and 5): From the TH treated samples only 22 out of 38 show clearly two components in the demagnetization diagrams. The HT-component is removed only above 500°C, but in this site the HT-component is best derived from temperatures higher than ~545°C. For 7 out of 12 AF demagnetized samples two components are clearly visible, with the HC-component in the range of 30-100 mT. Although only one sample has been demagnetized with the pc-method (LBC35), it appears that samples from the LBC-site have been less affected by a GRM than the other sites of the Hooggenoeg Complex.

LPB (Figure 4E, 5 and 6): The demagnetization diagrams of this site are less clear compared to the previous sites. At higher temperatures the data-points appear more scattered which makes it harder to interpret the HT-component. For 14 of the 31 TH-demagnetized samples a recognizable second HT-component was found. From the AF-demagnetized samples, 5 out of 7 give a HC component (from 40 up to 100 mT). This component is not recognized as GRM since it is directed towards the origin.

The 45° cut-off analysis is applied on the samples which pass the first step of the selection. Figure 7 shows the result for the HT component of the samples from sites MDI and LPB. Red dots in the diagrams represent samples which are cut-off by the program. As a second step in the selection of data these samples will be excluded for the interpretations as well. In the end, only samples which show clear two-components in their demagnetization diagrams and which are not excluded by the 45° cut-off will

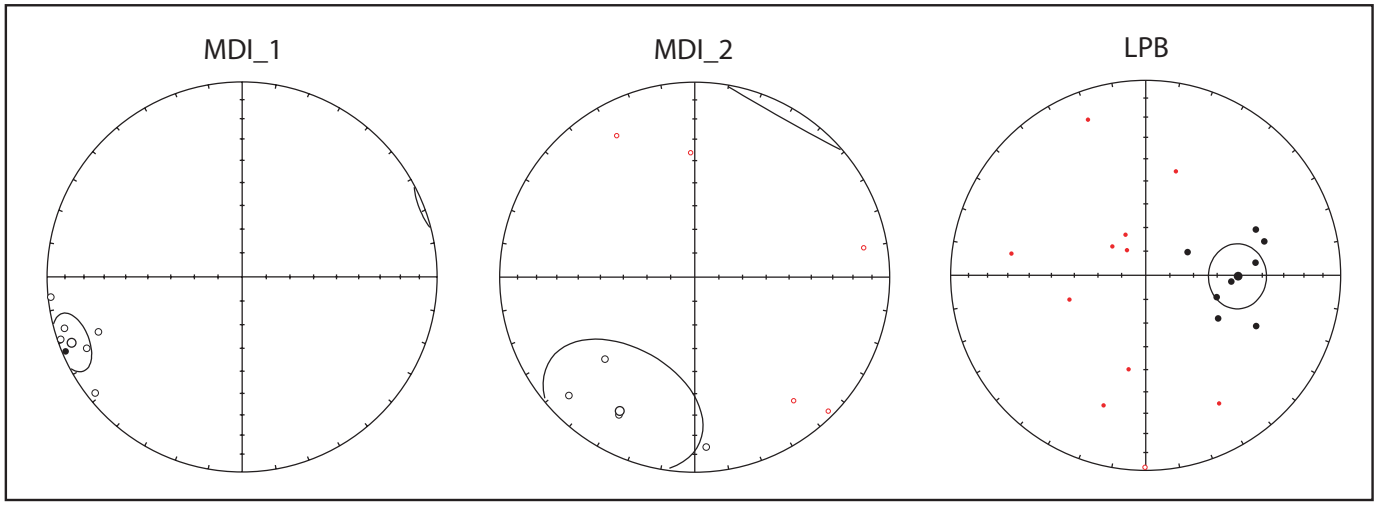

Figure 7

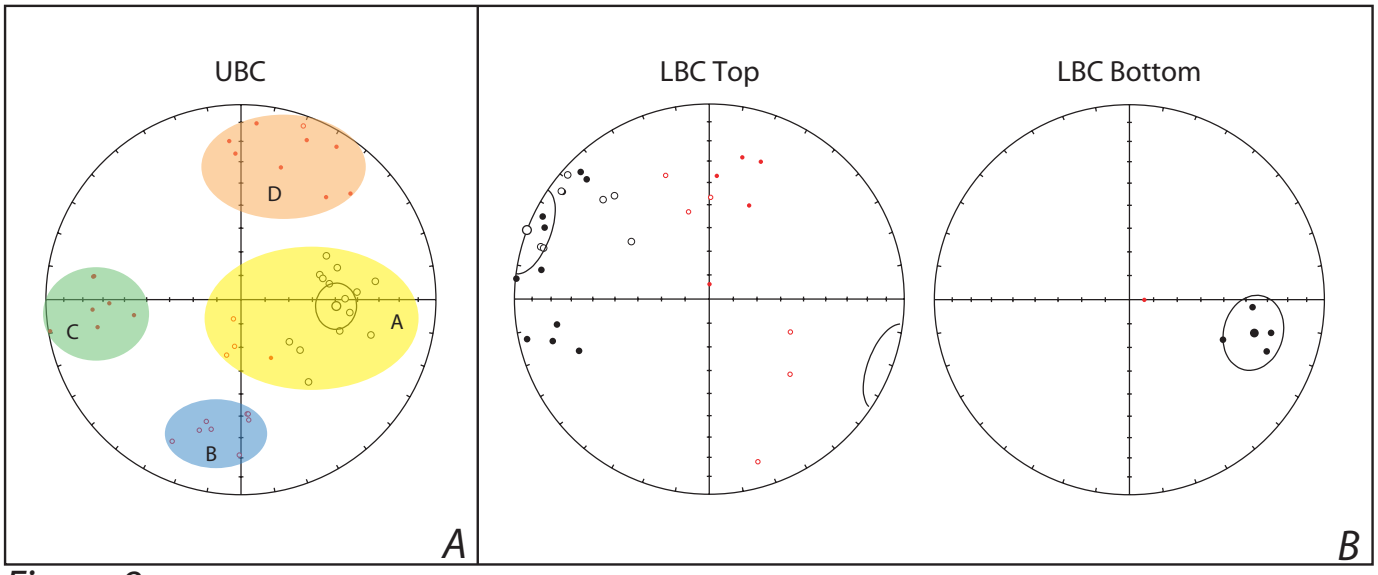

Figure 8

FIGURE 7. ChRM-diagrams (in situ) after 45° cut-off for sites MDI and LPB. Large circles indicate the error of the mean value, calculated from the black dots. Red dots are rejected samples by the cut-off. Filled (unfilled) dots representing the lower (upper) hemisphere.

FIGURE 8. diagrams (in situ) after 45° cut-off for sites UBC and LBC. A. In site UBC four clusters can be recognized in the diagram, one in the black dots and three in the red dots, resulting in a different interpretation of the diagram. Red dots won't be rejected but gathered separately in semi-sites. In the plot of site LBC (B) a division in the dots is visible as well, red dots cluster around the 90° declination-line, suggesting also two semi-sites present. For the plots of Figure 7 the red dots are rejected fur further interpretation.

be used for further interpretations.

Care must be taken however with the second step in the selection. For two sites the cut-off analysis gives more red dots than samples that are not cut-off. It seems that a stratigraphical correlation exists between the both cut-off samples and the non cut-off samples which appear in clusters. This is most clearly visible for site UBC. Four distinct clusters (A-D) can be recognized in the ChRM-plot (Figure 8A). Remarkably, these clusters are all stratigraphically determined in subsequent intervals, from the top of the section (cluster A) to the bottom (cluster D). Single ChRM-plots have been constructed for these four clusters which will be called semi-sites, with each semi-site giving a well determined direction individually. The four semi-sites of UBC will be used for further interpretation.

For site LBC the equal area plot of ChRM direc-

tions shows two clusters after the 45° cut-off. The cluster of red dots are samples from the stratigraphical bottom of the site and a single ChRM-plot is constructed for this cluster. A well determined direction is found for this bottom part of LBC (Figure 8B). This implies a shift in direction through the younger part of LBC to the older, bottom-part.

The mean direction of the bottom part of site LBC is similar to the mean direction found for site LPB (Figure 7). These two sites are stratigraphically connected, with site LBC more close to the diabase intrusion than LPB. This can suggest a shift in mean direction influenced by the intrusion. We note, however, that site LPB shows a large scatter in data and the mean is calculated from only 8 samples out of 19, since the other samples are excluded by the cut-off. This suggestion need to be investigated with a higher sampling rate for both the sides of the intrusion.

5.2 Great circle analyses

To find out if there is any consistent overprint direction in the low temperature (LT) and low coercive (LC) fields resulting from cutting the samples, a great-circle approach has been performed on the LT-components of the four Hooggenoeg Complex sites (Figure 9). All sites give very high errors for the great-circle determinations due to the large scatter of the LT/LC data. The best result is the great-circle determined for site LBC, giving a pole with declination 291.2 and inclination -27.9 but the maximum angular deviation (MAD) is too high to be of good use. This implies that the overall found pervasive LT/LC overprint is present but too random orientated to indicate the origin. Figure 10 shows the great-circle through the HT-components of the four sites of UBC. They roughly align on a great-circle. The dotted-line in the diagram represents the orientation of the possible overprint from cutting the cores. Both poles of the Karoo overprint and the GAD are plotted to compare, but no clear correlation is found.

5.3 Decay curves and Curie diagrams

Decay diagrams of all the three complexes are shown in Figure 11. There is no big shift or difference between the complexes; all diagrams show a range from multi component (several plateaus, or drops in intensity visible) to single component (one plateau) types. The single component diagrams show an almost constant intensity for most of the temperature range followed by a big drop at temperatures higher than 500°C: this is likely due to fine-grained (PSD or SD) grains in the specimen. The drop in intensity seen in most of the samples at 20°C, is due to the treatment with N_2 to remove the LT-component. The amount of decrease differs from sample to sample. Steps in the decay curves indicate the presence of multi-components in the sample. Combined with the result of the Curie-diagrams these components can be determined. One important common feature in most diagrams is the sudden large decay from 500°-590°C. This is similar to the temperature-range of the HT-component in the demagnetization diagrams. Intensities are reduced to zero around 580°C, which indicates the presence of magnetite in the samples. This can be confirmed by the Curie-diagrams of 11 samples in and near the diabase intrusion in the Hooggenoeg Complex. These samples are selected by their position relative to the diabase intrusion in the so-called 'baked-contact': samples UBC 02 and LPB 05 come from unaltered/unbaked country rock, UBC 19, 36, LBC 69 and 97 are altered pillow basalts in the contact aureole of the intrusion, sample UBC 42 comes from what is believed the real baked contact itself and samples MDI 1-2, MDI 2-9 and LBC 42 come from the diabase intrusion (Figure 12). Some diagrams are scattered due to low intensity and background noise, and these cannot give clear indications on the magnetic carriers. Most diagrams, for example UBC 42 and 50, show a very clear Curie-point around 580°C, which points to magnetite. The Curie-diagram for UBC 36, shows a drop in total magnetization around 350°C: an indication for maghemite.

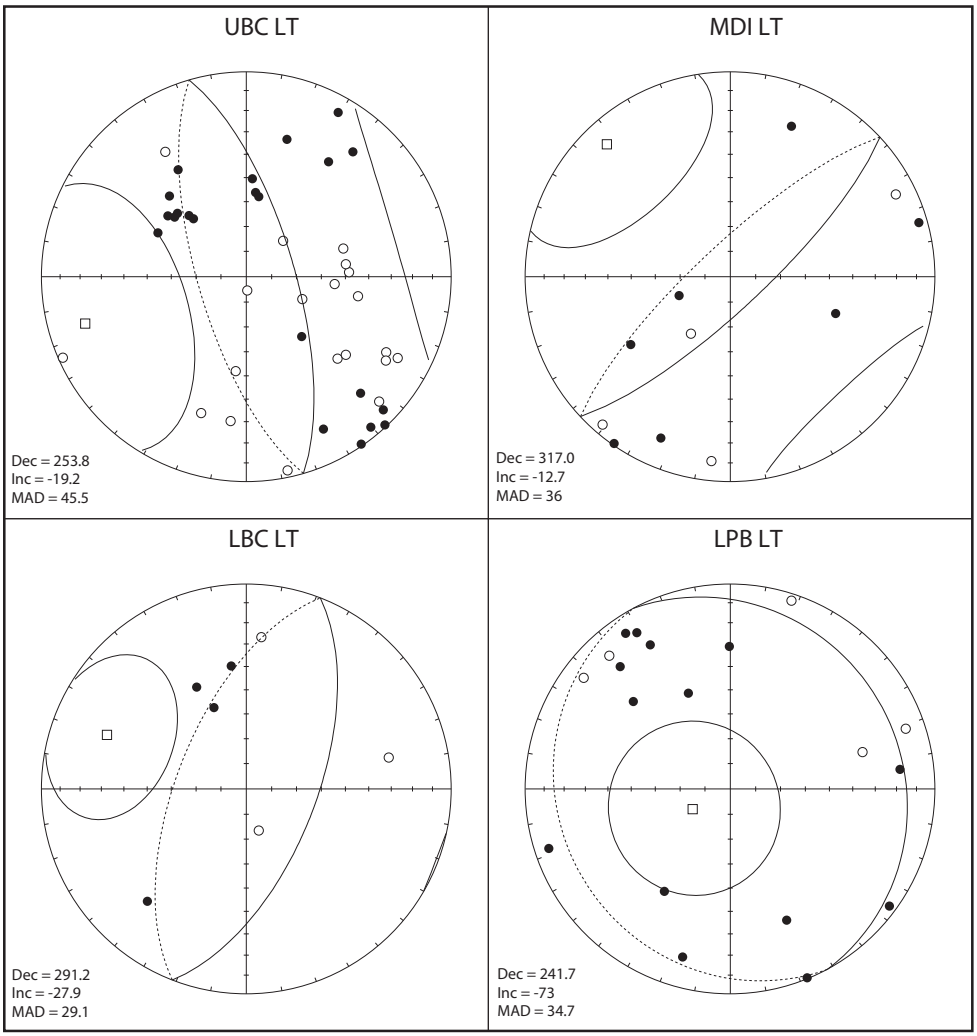

FIGURE 9. LT-component great-circle plots for all four Hooggenoeg sites. Poles of fitting great-circles give very high MAD's, indicated by the circles around the pole-plots. Declination, inclination and MAD for the four poles are indicated in the left bottom corner of the diagrams.

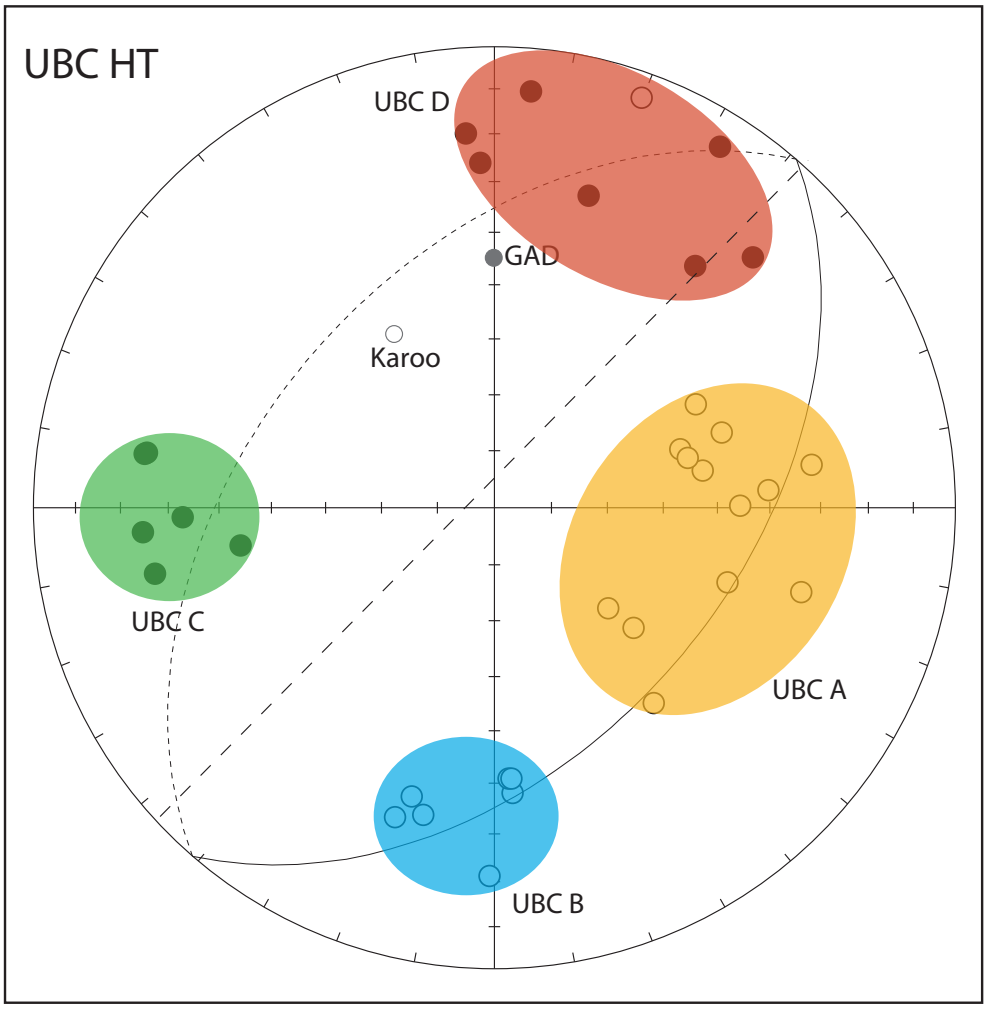

FIGURE 10. HT-component great-circle plot for site UBC. Semi-sites are indicated in different colors, showing a shift in direction from A - D. Dashed line indicated the orientation of the saw-table overprint (337/45) for hole KD2. GAD and pole of the Karoo event are plotted to compare with the found directions.

Mendon Complex (Ncakini Fm)

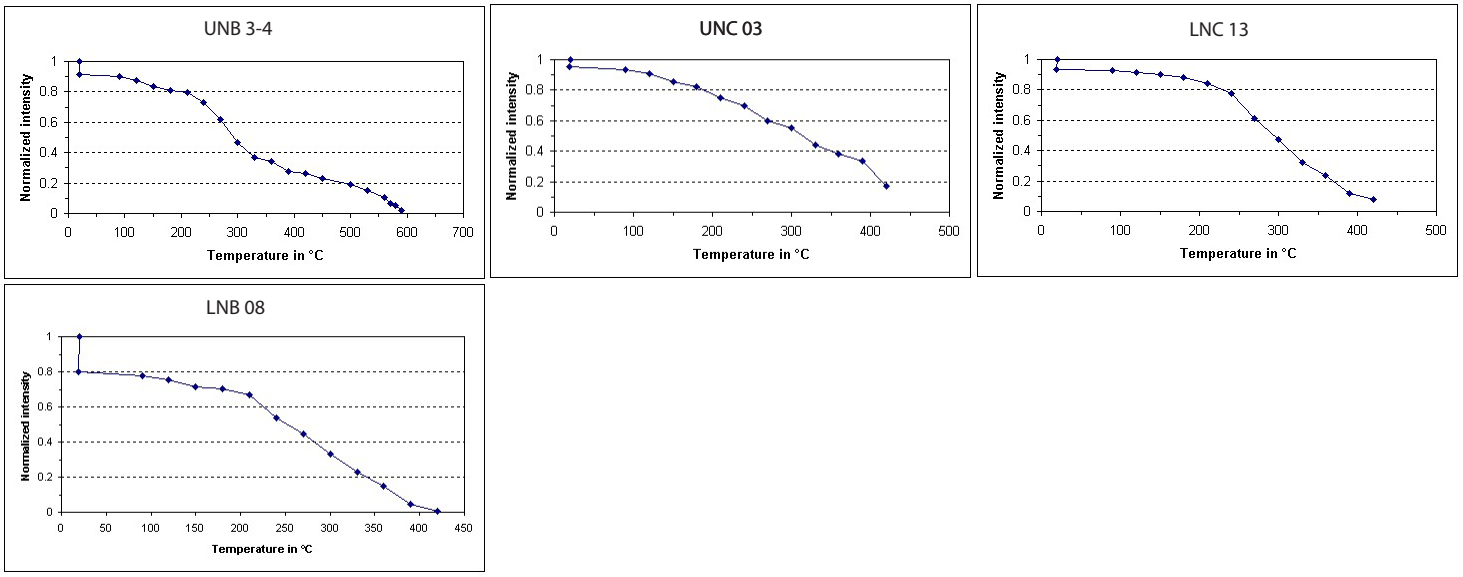

Noisy Complex

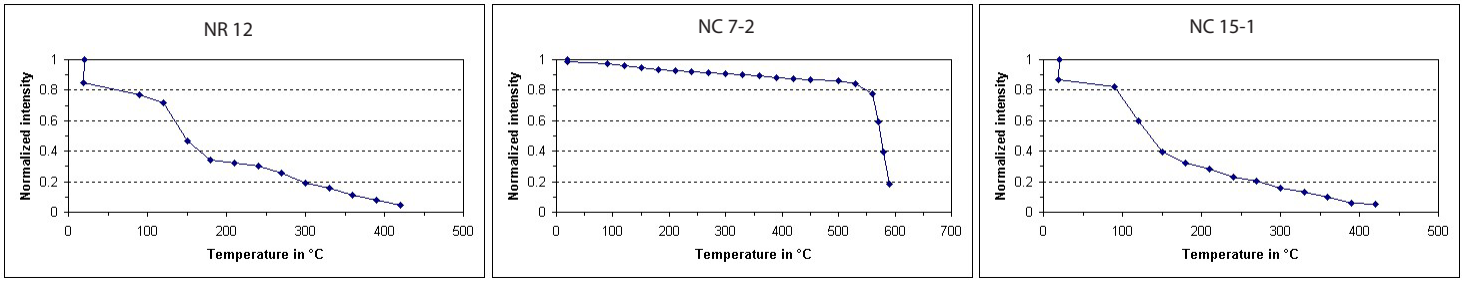

Hooggenoeg Complex

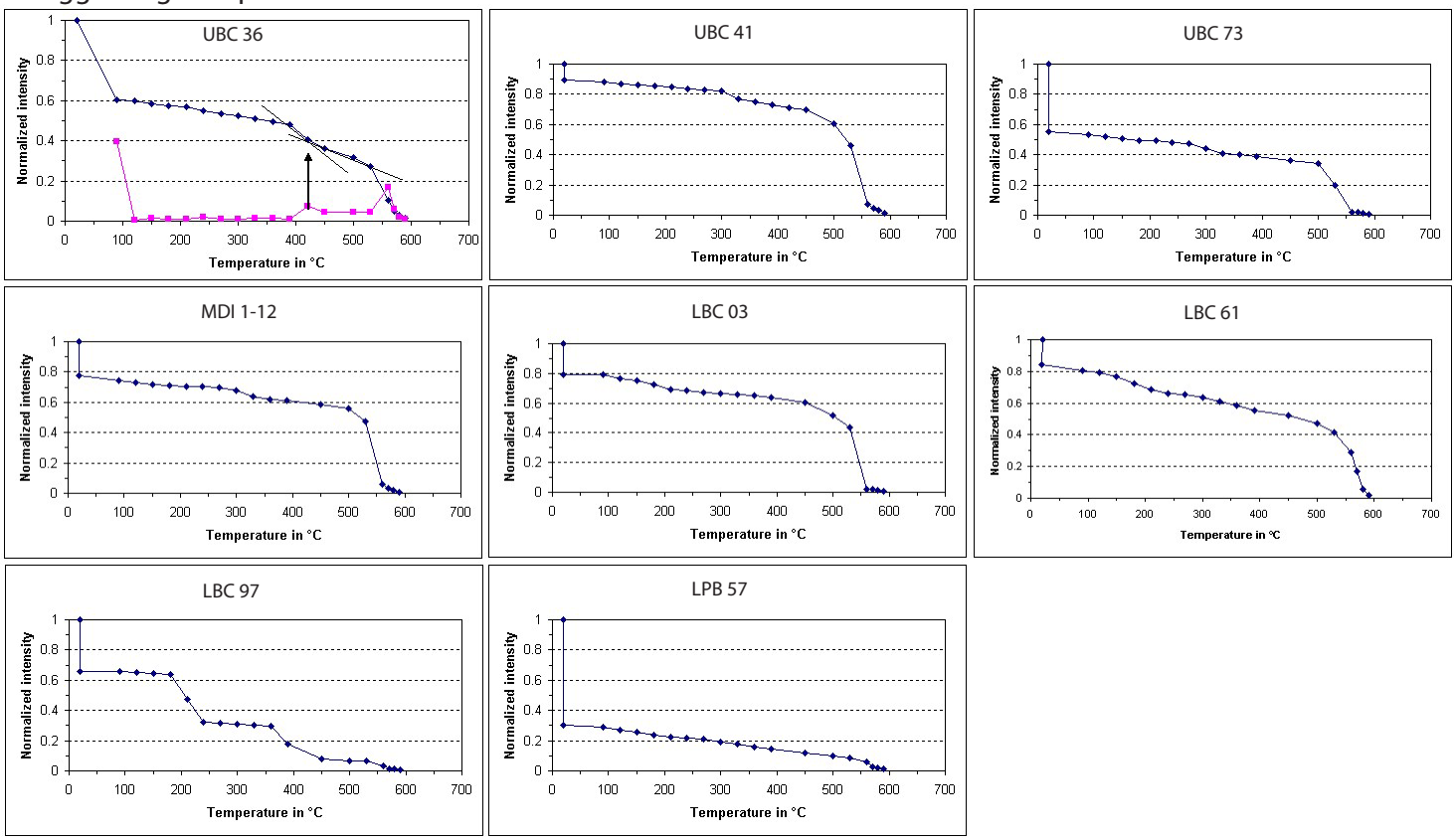

FIGURE 11. Decay diagrams from TH-demagnetization per site. Large decay from the first to the second dot is due to the AF- or N2-method. Samples with a plateau followed by a large drop in intensity contain SD-grains. Different components can be recognized by different plateaus visible in the decay diagrams. In diagram UBC 36 difference in decay is indicated by the purple-pink plot, indicating the presence of maghemite from the jump around 350-400°C. Magnetite is indicated by the large decay-drop near

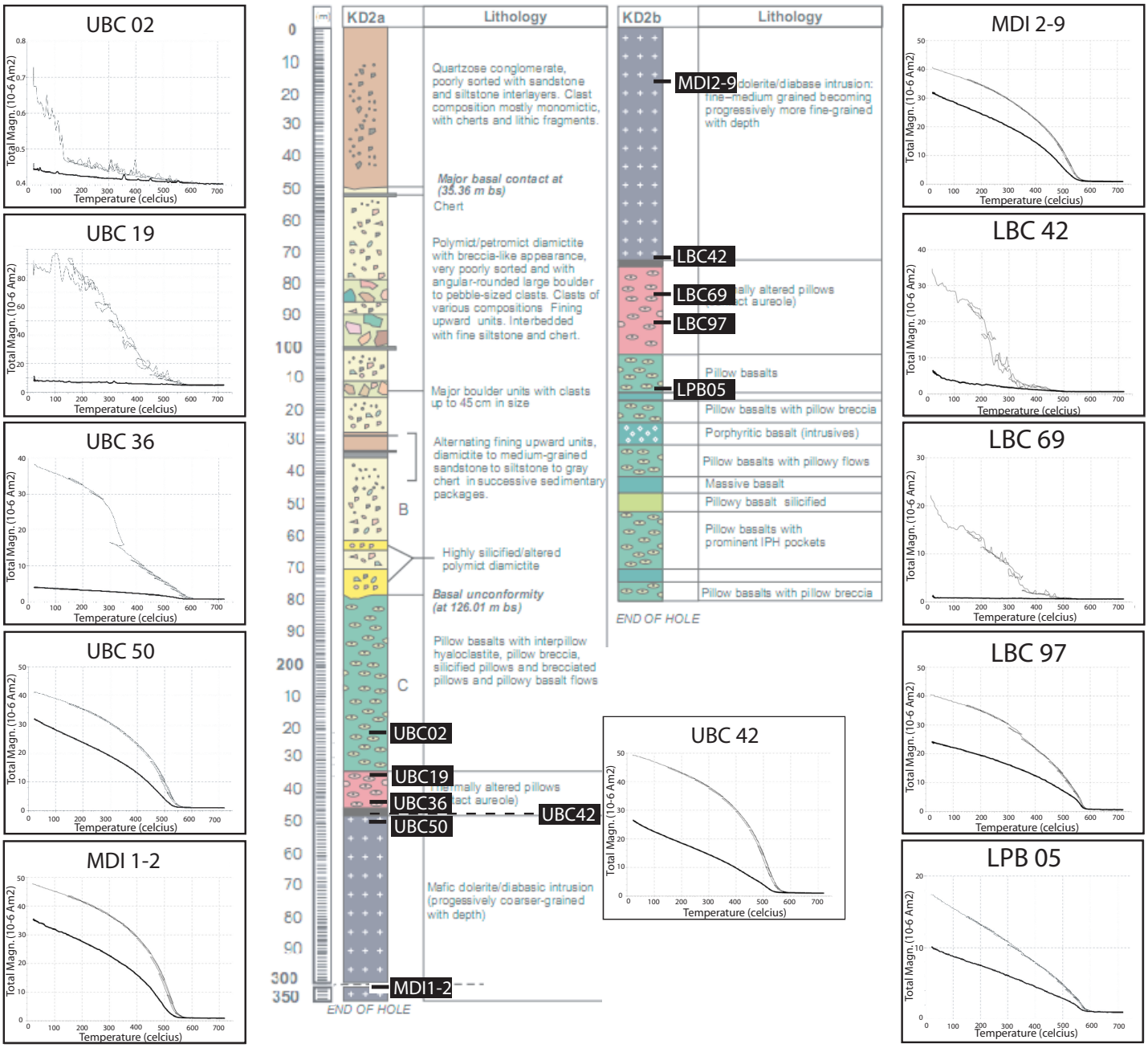

FIGURE 12. Curie-diagrams for samples in the baked-contact in the Hooggenoeg Complex. Sample positions indicated in the stratigraphic column from Grosch et al. (2009). Most samples show clear Curie-points around 580°C, representing the presence of magnetite as main magnetic carrier. Drop in total magnetization around 350°C in diagrams of UBC 36, LBC 97 and LPB 05 indicate conversion of some amount of magnetite to maghemite. Sample 42 is taken in the upper baked-contact itself, with magnetite as main carrier.

The Curie-points for LBC 42 and LBC 69 are shifted to some lower values (around 500°C). This can be explained by the presence of (titano) magnetites of different compositions, as is often found in basalts. There is no clear evidence for a shift in magnetic carriers through the baked contact. However, indications for maghemite, although not as pronounced as in UBC 36, can be found in the diagrams of LBC 42, LBC 69 and very slightly in LBC 97. This implies the presence of maghemite, concentrated around the baked contact. Indeed, from Figure 13A it can be seen that the magnetic carrier in UBC 36 is likely small-grained maghemite when it is compared to the characteristic thermomagnetic curve for maghemite from de Boer (1999). Figure 13B shows decay-diagrams from Dankers (1978) for different grain-sized maghemites. All diagrams show two decay intervals (resulting from the inversion to hematite): the first interval is between 100°C and 350°C and the second between 350°C and the (unknown) Curie point

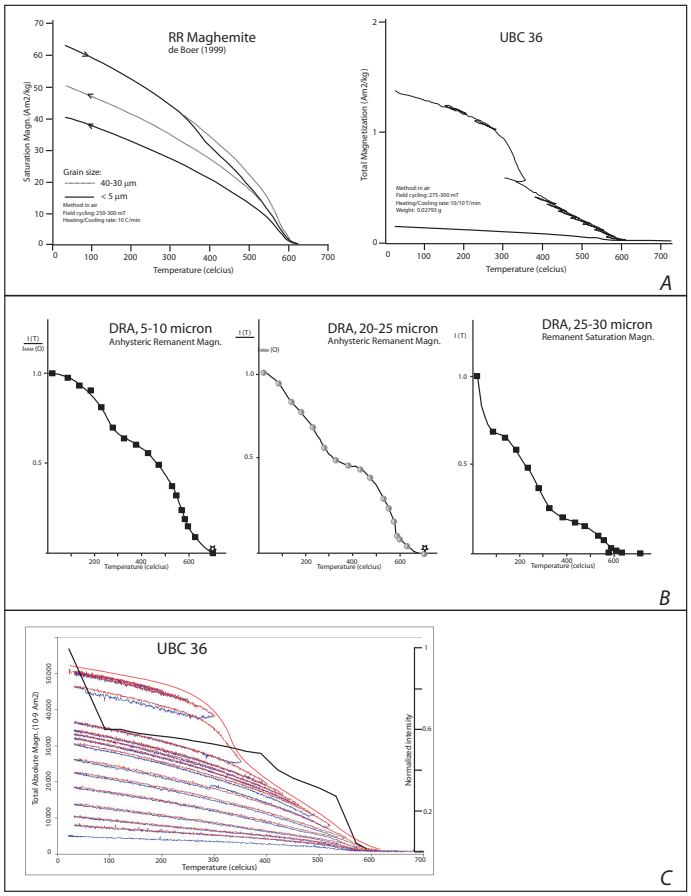

FIGURE 13. A) Simplification of a diagram for maghemite after de Boer (1999) compared with the simplified Curie-diagram of sample UBC 36. Small grain-sized maghemite is responsible for the drop around 350°C in sample UBC 36. B) Simplification of maghemite normalized diagrams from Dankers (1978). Three components in the diagrams are characteristic for maghemite as magnetic carrier. C) Curie-diagram for sample UBC 36 with temperature loops back to 20°C for each step. Black line represents the decay-curve for the same sample (right axis showing the normalized intensity for this curve). This diagram can be compared with A and B to indicate the presence of maghemite in the sample.

of maghemite (Dankers, 1978). Discussion can be made about the determination of the Curie point of maghemite but this is out of scope for this research. The two decay interval components from Dankers (1978) can be related to the two components in the decay-curve for UBC 36 (Figure 13C). The low temperature drop of the 25-30 micron diagram from Dankers (1978) must not be confused with the low temperature drop in the decay-curve of UBC 36; this intensity drop is the result from the N_2-procedure to remove the overprint. The division of temperature intervals can be recognized in the extended Curie-curve for this sample as well (with temperature loops back to 20°C, Figure 13C). Points of difference in magnetization appear very close to the boundaries of the two components in the decay-curve, especially for the 350° component. The end-temperature is lower for sample UBC 36 than for the samples of Dankers (1978). This can be explained by the fact that UBC 36 does not exist of pure maghemite but of other (titano) magnetites as well (probably a large amount of magnetite which is not completely converted to maghemite).

5.4 Conglomerate test

A combined conglomerate test has been performed on seven samples from the Noisy Conglomerate, all from different clasts. We used both the Shipunov test and the Watson- (randomness) test. We tested four different reference values: one is the PDF (342/-63), another is the Karoo overprint (330/-53) (from Biggin *et al.*, 2011); and two new values: the LT-component determined from 5 conglomerate samples of the same site (51.6/-20.3) and the GAD (0.0/-44.3). The Watson-test results are positive for all reference values, but the Sipunov-test is negative for all the reference values (Table 4 and Figure 14). The Shipunov-test with the LT-component as reference value is the least negative. One must take into account that the number of samples used for the tests is too low for firm conclusions. Since both Usui *et al.* (2009) and Biggin *et al.* (2011) find a positive test for the Noisy conglomerate, clearly more samples should be used for this test here.

N	Ref. value	R0	R	Rho0	Rho	Result Watson	Result Shipunov
7	342/-63	4.18	3.602265	0.362	0.453321	R < R0	Rho > Rho0
	PDF					positive	negative
7	330/-53	4.18	3.602265	0.362	0.398478	R < R0	Rho > Rho0
	Karoo					positive	negative
7	51.6/-20.3	4.18	3.602265	0.362	0.382252	R < R0	Rho > Rho0
	LT-component					positive	negative
7	0.0/ -44.3	4.18	3.602265	0.362	0.437392	R < R0	Rho > Rho0
	GAD					positive	negative

TABLE 4. Overview of the conglomerate test with different reference values. All runs performed with 7 samples. R0 and Rho0 stand for reference values, R and Rho for measuered values for the Watson and Shipunov tests respectively. Reference values are: 1st test – PDF from Biggin et al. (2011), 2nd test – Karoo overprint from Biggin et al. (2011), 3rd test – LT-component (n=5) of site NC of this study and the 4th test – GAD.

5.5 Data overview Hooggenoeg Complex sites

Figures 15-18 show data overviews of the four sites of the Hooggenoeg Complex. For each site the Curie-diagrams, declination/inclination plots and ChRm-plots are placed around the stratigraphic column. The ChRM-plots show all the data-points after the first selection, the declination and inclination plots show the directions after the second selection (black dots in the ChRM-plots). Declination and inclination data points are plotted with respect to the stratigraphic column for a good overview of possible trends through a section. It is important to realize that all data are not tilt corrected (no tc) in this whole study.

For the UBC site (Figure 15) it is immediately clear that a shift through the section is present. This is indicated with the different colours for the different semi-sites A-D. From young to old, four shifts in both declination and inclination are found. This can be explained by a possible influence from the heating contact of the intrusion. The direction from UBC A acts in that case as the reference value for the country rock around the intrusion, and the values from B-D stand for the igneous rock. Sample UBC 36 with maghemite content is positioned in UBC A, near the boundary between country and igneous rock (see Figure 12).

The two sites in the middle of the intrusion (MDI 1 + 2), show a small shift in mean ChRM-directions (Figure 16). A large scatter in ChRM-data results from only 4 data-points for the dec/inc plots of MDI-2. No differences in the Curie-diagrams can be found, for both sides it is clear that magnetite is the main magnetic carrier.

As already mentioned the ChRM-plot for the LBC site (Figure 17) can be divided in a top or main part and a bottom part. The bottom part has only 4 data points which come through the sample selection, but their mean is very well determined. Remarkable is the shift in declination of nearly 180° in the middle of the altered country rock in the contact aureole of the intrusion. In the bottom part some maghemite is present. This is very comparable with the next site LPB (Figure 18). In the top, near the bottom of LBC, some maghemite is found in the Curie-diagram. The ChRM-mean value is very close to the value of the bottom of LBC.

6 Discussion

6.1 Sample handling and methods

6.1.1 Overprint removal

The NRM intensities of the sampled sites are generally in the same range of other studies (e.g. Biggin *et al.*, 2011: 1-100 mA/m). However, the maximum values for many samples from the Hooggenoeg Complex give very high values up to 17 A/m (Table 2): orders of magnitude stronger than expected for these Archean basalts. Since the fresh rocks of this study cannot be affected by lightening, another external factor must be responsible for the introduction of these high NRM-values. At the beginning of sampling the core we already observed that the cutting-table, which was used to cut the cores in half, the cutting-blade and the gutter are extremely magnetic. The strength of this magnetic field can be compared with the strike of lightening, introducing a strong overprint signal (isothermal remanent magnetizaton: IRM) in the samples. Since all cores were cut on this table, no comparison can be made with other samples to exclude the NRM introduction from the cutting-table. Since this large overprint has shown to be of large influence in many samples, it can be concluded that due to the unfortunate use of strong magnetic material during sampling a large amount of the possibly primary signal has been destroyed. For future studies this should be an important point of caution.

Two methods (N_2 and AF) have been used to minimize the overprint signal with minimum destruction

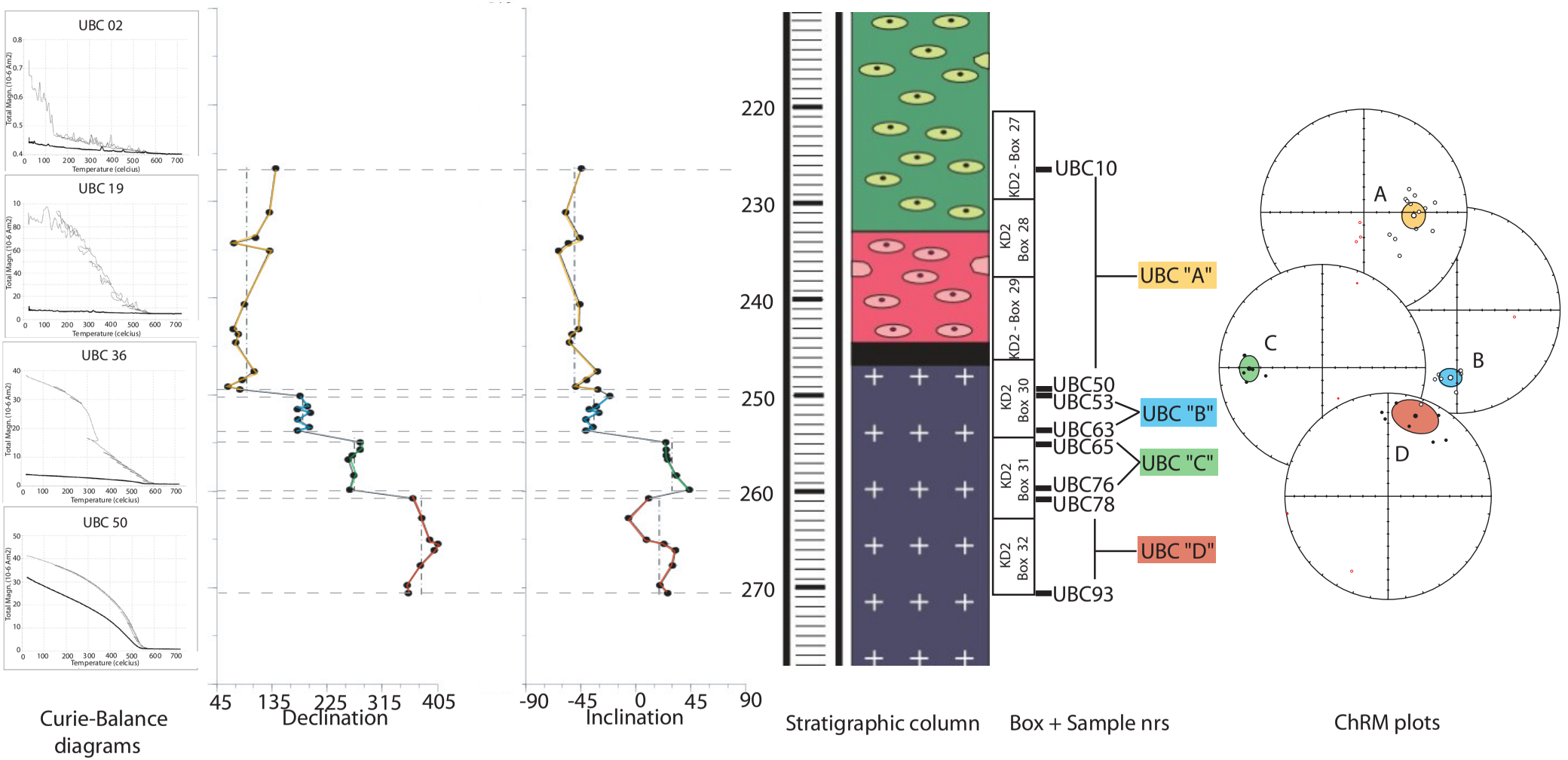

FIGURE 15. Overview of data for site UBC. Semi-sites A-D are indicated with different colors. Same colors refer to the semi-sites in the declination and inclination plots, showing a shift in direction from semi-site A to D. Dashed lines in the dec/inc plots indicate mean values for the directions. Errors of data points in the dec/inc plots are indicated with horizontal lines inside the dots. Stratigraphic log from Grosch et al. (2009) with positions of the different boxes to the right. ChRM-plots are in situ.

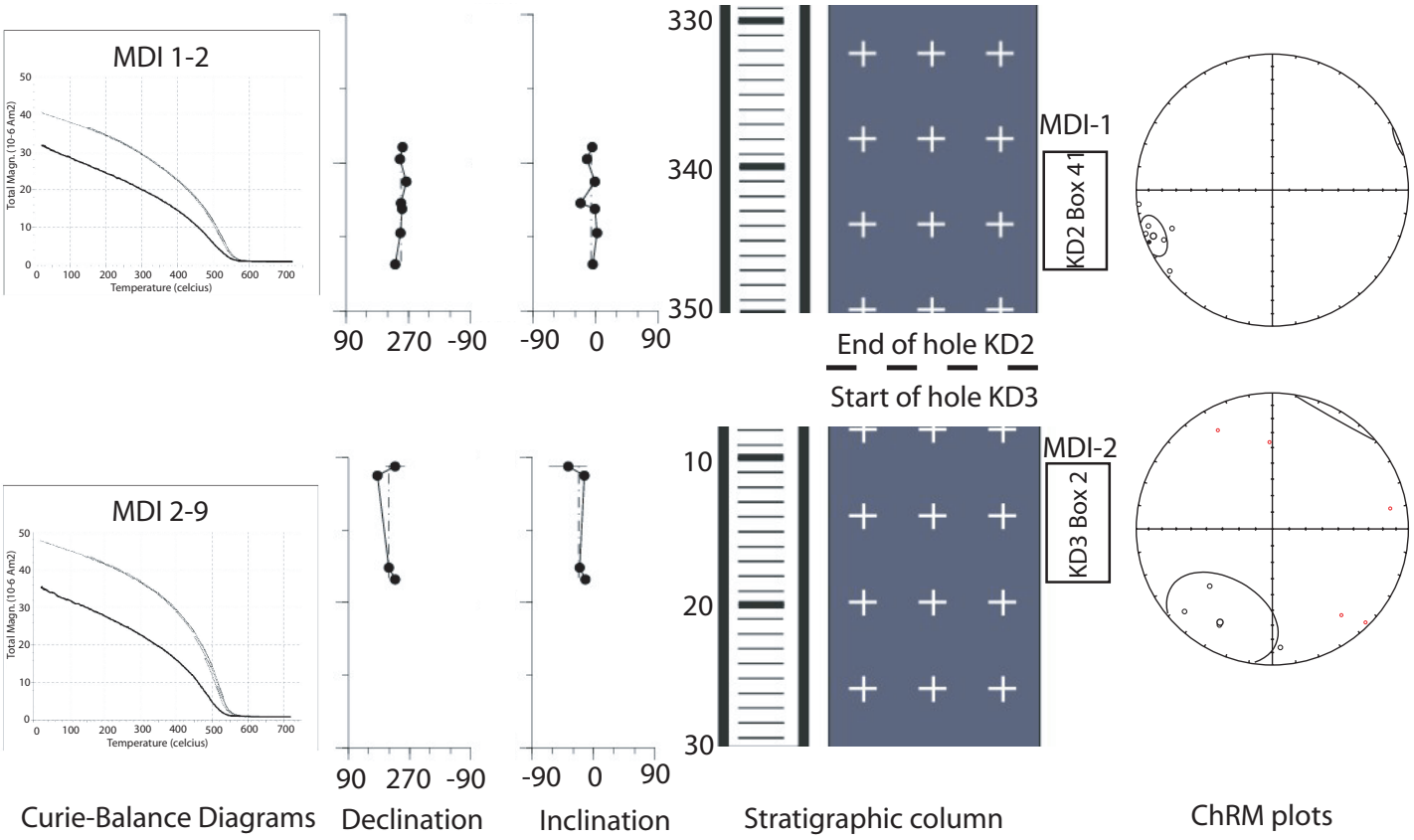

FIGURE 16. Overview of data for sites MDI 1 and 2, symbols and indications as in Figure 15. MDI 1 is located in the end of hole KD2, MDI 2 at the start of hole KD3, both inside the intrusion. A shift in mean direction from MDI 1 to 2 is visible from both ChRM-plots and dec/inc plots.

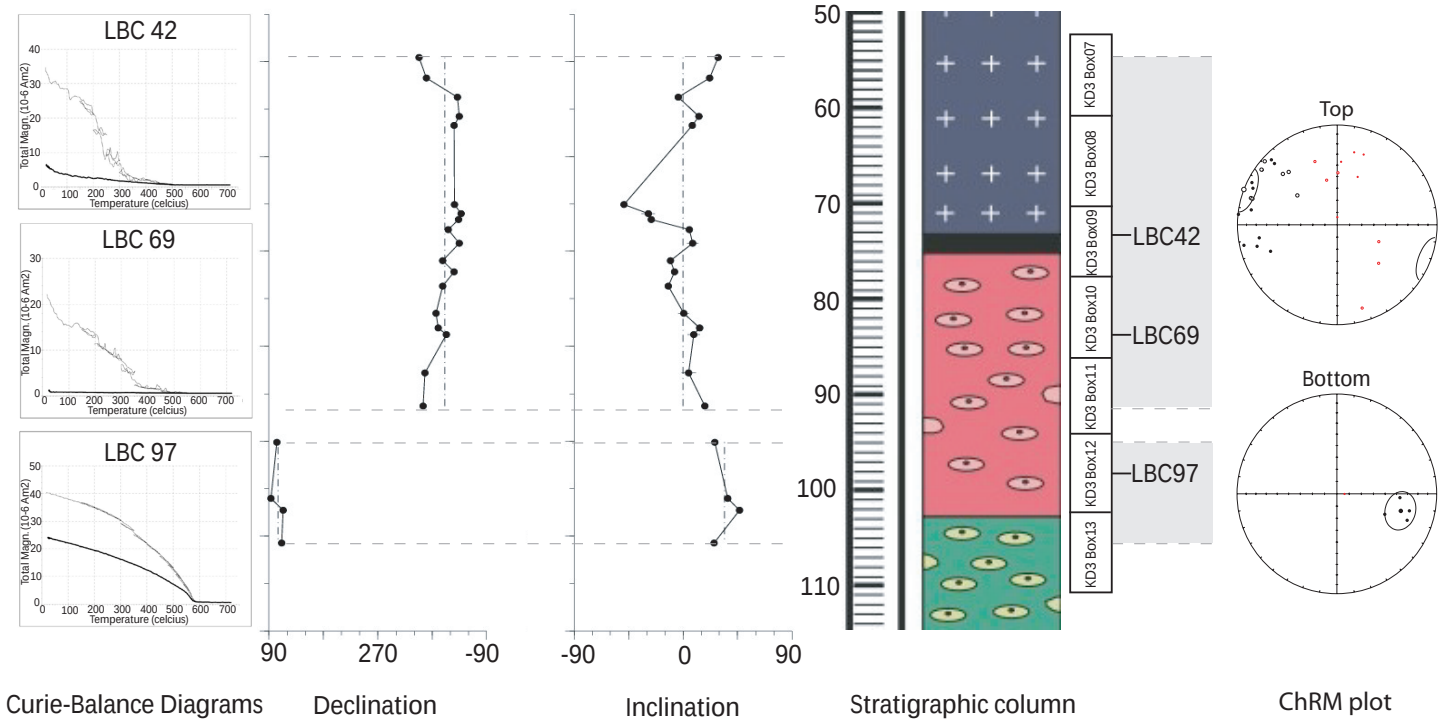

FIGURE 17. Data overview of site LBC, symbols and features as in Figure 15. Grey boxes right of stratigraphic column represent the top/main part and the bottom part of the site as interpreted from the 45° cut-off. ChRM-plot of the bottom part is similar to semi-site UBC A and of site LPB.

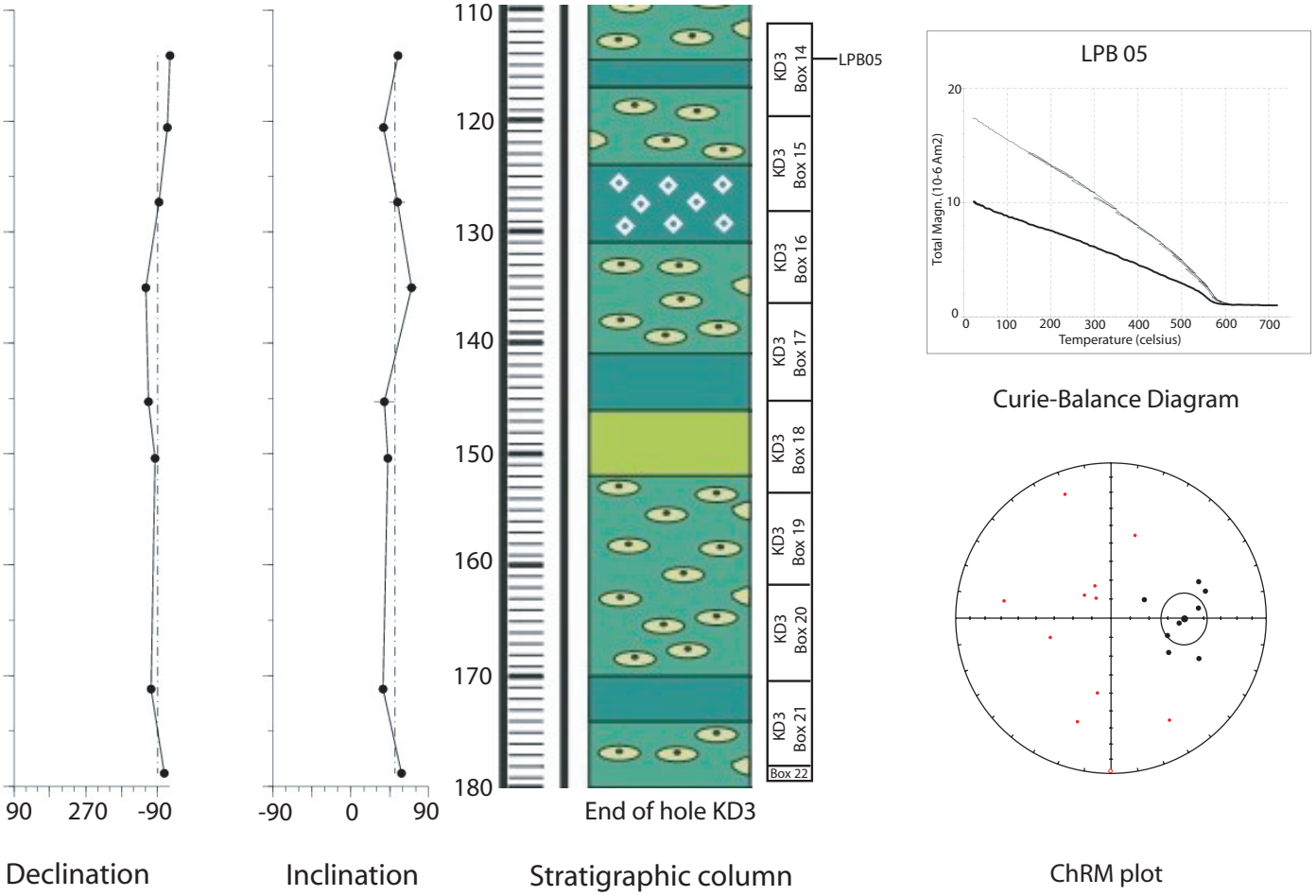

FIGURE 18. Data overview of site LPB, symbols and features as in Figure 15. ChRM-plot shows the large rejection of data points by the 45° cut-off. Dec/inc plots show a constant direction for the non-rejected samples, which is in the same direction as the bottom part of LBC.

of the (near-) primary signal. The treatment with N_2 seems to give the highest reduction in intensities compared to the small-step AF-demagnetization. However, interpretation of the demagnetization diagrams shows a LT-component up to 300°C, and even up to temperatures higher than 500°C. In various samples this LT-component is recognized as one single cluster: no removal of intensity is seen (Figures 4 and 11). 80 TH-demagnetized samples have not been treated with the N_2- or AF-procedure and gave comparable demagnetization diagrams, often showing the same LT-clusters. In many cases, the overprint signal is too strong to be removed completely by any of the methods examined and useful breakdown of magnetic signal only starts at temperatures higher than 300°C up to 500°C. When any more samples of the same BSDP-cores will be used for paleomagnetic research it is therefore suggested to use large TH-increments up to 300°C without using valuable time on one of the other methods.

6.1.2 Measurements and sample-selection

Measurements on the samples from the BSDP-cores can best be performed with TH-demagnetization. AF-demagnetization gives comparable results, but in many samples a GRM is introduced and the more time-consuming pc-method should be used for best results. Secondly, the overprint signals are not as clearly separated in the AF-demagnetization diagrams as in the TH-diagrams. The data of the LT-component of the studied samples give no clear directions; a consistent overprint direction introduced by the cutting of the samples as stated earlier is not separated clearly. Possibly, even all the primary signal is overprinted and destroyed in the studies samples. For any new samples from the studied complexes an overprint should be avoided, because important information is lost with demagnetization and interpretation of the primary signal can be very difficult.

The final step for the best handling of the samples from the BSDP cores is a careful selection of the samples used for analyses. A double-selection should be performed. First, the samples should be selected on their demagnetization-diagrams; clearly different LT- and HT-components must be recognized. If no clear difference is seen, samples are not reliable since it is not clear which component is being interpreted: probably only the LT-component is removed in these samples. Secondly, the use of the 45° cut-off method is necessary to exclude samples which are scattered from the mean. The 45° cut-off can be used to identify clusters in sections as well, which may result in better interpretation and understanding of the data.

6.2 LT- and HT-components

From the Mendon and Noisy Complex, 87 and 68 samples have been taken respectively. Since test samples gave scattered demagnetization diagrams which were difficult to interpret and intensities of these samples were the lowest from the whole section, these complexes are believed to be most influenced by the large overprint. Further study on these complexes was rejected due to this absence of any leftover primary signal. A better intensive study on these two complexes on new samples, from surface studies or new drilling studies, require better results if no disturbance of any external magnetic field is implied. Higher and better intensity results from samples of the Hooggenoeg Complex gave rise to the focus on samples from this complex in further steps of this study. Hope is on finding indications for a (near) primary signal in these samples.

LT-components from sites UBC, MDI, LBC and LPB do not give an overlapping or consisting result. No clear conclusion can be made for the interpretation of these LT-components since they give scattered results (Figure 9). If the overprint is introduced by the cutting of the samples, we expect to find a direction related to the drilling direction of the cores (317/45 for samples from cores KD1 and KD2 and 337/43 for KD3) for the LT-component. However, this was not the case. A random LT orientation was found with no consistence with other studies like Bigging *et al.* (2011). An explanation of this lack of a clear LT-direction cannot be found and should be solved with more studies on new cored samples.

A shift in direction of the HT-components of semi-sites UBC A-D could be explained in terms of their geological setting, since it is expected to find a shift in direction through a baked-contact from country rock to igneous rock: from UBC A-D in this case respectively. This is observed close, but not at, the baked-contact (Figure 15). The primary origin of the HT-components is however uncertain as argued above. This can be tested by comparing the baked-contact at the other side of the intrusion, in site LBC. A shift in direction is recognized in this site as well from top to bottom, but similar with semi-sites UBC A-D only in the host rock and not at the contact as defined in the stratigraphic column (Figure 17). The bottom mean direction has a similar declination as UBC A, but the inclination is of reversed sign. In the country rock, in site LBC, a remarkable similar mean direction is found compared to the bottom part of LBC: a similar declination but reversed inclination than semi-site UBC A. A shift in direction with respect to the intrusion is suggested at this site of the intrusion as well.

When the mean directions for sites in the intrusion (UBC B,C,D and MDI 1 + 2) are compared to each other, a large scatter is found throughout the whole intrusion. Probably not all the overprint signal has been removed with the methods used since the difference in directions is too big for secular variation. However, if the period of cooling the intrusion was long enough, in the sense of plate tectonics, this could be an explanation. A more intensive study on the plate tectonics and this particular intrusion is needed to find the answers to this problem.

6.3 Conglomerate test

For site NC a conglomerate test has been performed with four different reference values. Clearly more samples than now used should be included which will improve the test. None of the used values gives a positive result for both the Watson- and Shipunov-method, only the Shipunov-test with the LT-component of the conglomerates as a reference value is close to positive (Figure 14). A very low number of samples (n=7) is used in this study for the test. Therefore, we must refrain from making firm conclusions from the tests performed in this study. We know from previous studies (Biggin *et al.,* 2011, Usui *et al.*, 2009) that the conglomerates from the Noisy Complex are suitable for a conglomerate tests when using a larger number of samples.

6.4 Comparison with other Archean paleomagnetic studies

The best samples from this study which can be used to compare with earlier published paleomagnetic research on the Onverwacht Suite come from site UBC. Data on these rocks is sparse, but Biggin *et al.* (2011) give a good summary on the data available (Figure 3, 4 from *Biggin et al.*, 2011). Biggin *et al.* (2011) recognized three temperature groups: a low temperature LT group divided in LT 1 up to 250°C and LT2 (removal between 100°C and 440 °C); a medium temperature MT group observed between 370°C and 480°C, and a high temperature HT group separable in cluster HT1 (isolated above 340°C) and cluster HT2, observed at temperatures > 460°C. In Figure 19 we plot the LT1 (Figure 19A) and HT2 (Figure 19B) components of Biggin *et al.* (2011) together with the mean HT-component directions from sites UBC (divided in the semi-sites A-D) and MDI 1. Additional the mean direction from Usui *et al.* 2009) re-examined by Biggin *et al.* (2011) is plotted as well ('Usui' in Figure 19) and the mean direction from the Noisy Formation Tuff (NfT) from Biggin *et al.* (2011) which is suggested to hold a (near) primary signal . The mean direction for 'Usui' is calculated from data from dacitic intrusions from the Noisy Complex (ages: 3438 ± 12 Ma, 3445 ± 8 Ma, 3445 ± 3 Ma and 3451 ± 5 Ma, see for details Usui *et al.*, 2009). No clear overlaps in directions from the combined studies is found. The overlap of mean directions of UBC C and 'Usui' is deceptive: the samples from this study and from Usui *et al.* (2009) are taken from the two different flanks of the Onverwacht Anticline. Since the mean directions plotted in Figure 19 are in situ, data from both flanks are expected to give completely different directions after tilt correction. Therefore, the (near-) primary signal from UBC C is not reliable assuming the data from Usui *et al.* (2009) are primary. It is noticed that semi-site UBC B plots near NfT which holds samples from the Noisy Complex. Since UBC B is part of the intrusion this can imply a common overprint if both signals are indeed (near) primary. However, problems arise since this possible correlation is only seen for NfT and would be expected in other complexes as well and the reliance of UBC B holding a (near) primary signal is discussable.

From all this the following hypothesis can be made: samples from the Hooggenoeg Complex are likely too much influenced by the overprint despite the double-selection procedure. The LT-component overprint found in all samples from this study is removed successfully, hence another overprint may remain. No overlap with one of the overprint directions from Biggin *et al.* (2011) is found, except for NfT with UBC B. The restriction in the amount of data gathered in this study makes it difficult to reconstruct more hypotheses on better constraints. However, despite of a large, external, present overprint from the cutting of the samples, some indications for a consistent HT component in samples from the Hooggenoeg Complex should stimulate further work on these rocks, if care is taken to avoid any magnetic contamination.

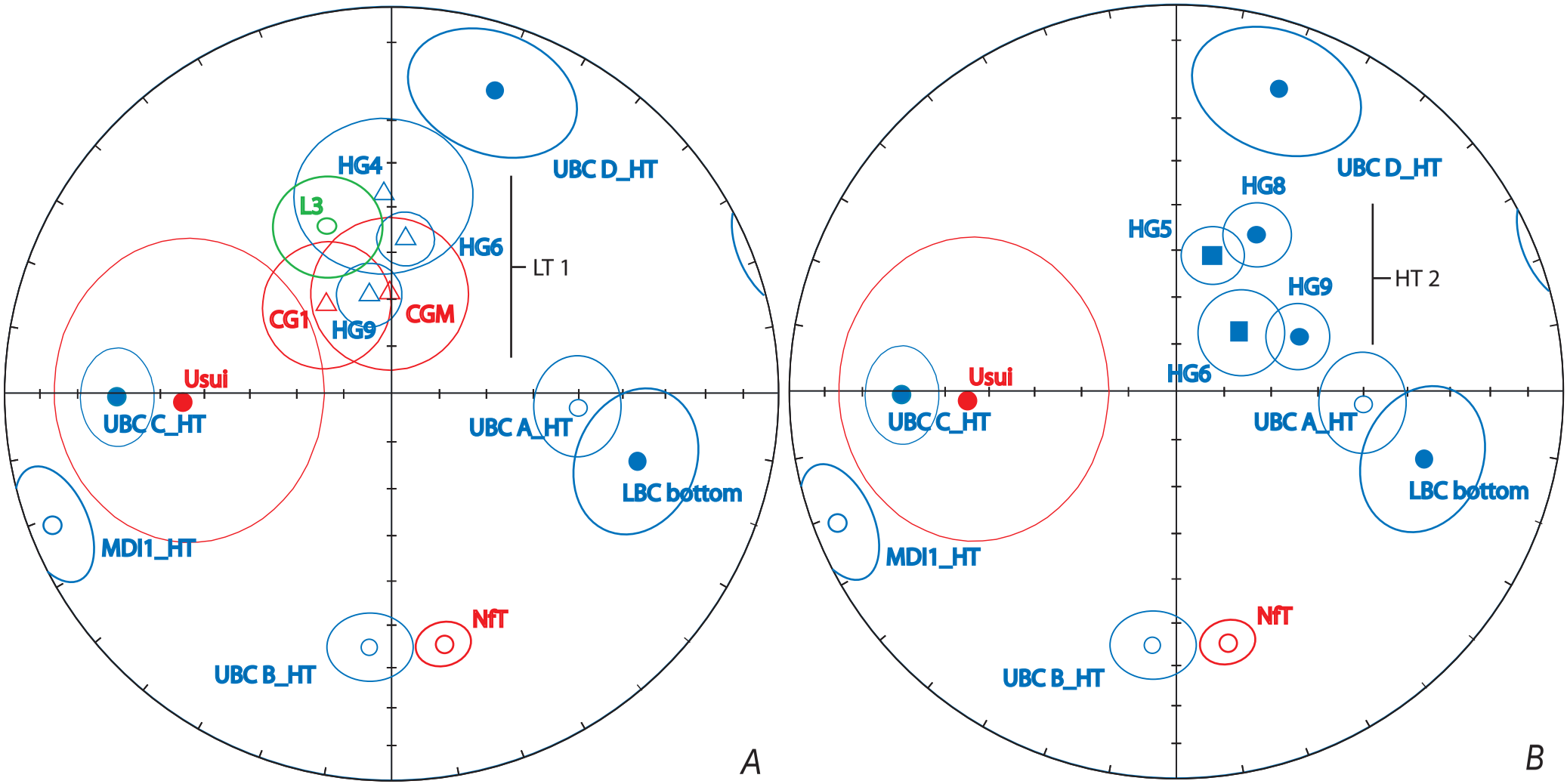

FIGURE 19. ChRM-plots of combined data. Blue indicates sites from the Hooggenoeg Complex, red from the Noisy Complex and green from the Kromberg Complex. A) UBC A-D and LBC bottom from this study (all HT). Low temperature components from Biggin et al. (2011) grouped in the region 'LT1' and include: HG4, HG6, HG9, CG1, CGM and L3 plus a plot of NfT . From Biggin et al. (2011) and Usui et al. (2009) 'Usui' is taken. Filled (unfilled) symbols represent lower (upper) hemisphere. B) Same plot as for A only LT1 group from Biggin et al. (2011) is replaced by the 'HT2' group with HG5, HG6, HG8 and HG9. No clear overlap can be found from both figures, only a near presence of UBC B to NfT. See text for detailed explanation.

7 Conclusions

New paleomagnetic data on fresh deep-drilled rocks from the Onverwacht Suite (ca. 3.55-3.3 Ga) have been presented in this research. These data are unique since no surface processes have been of influence on the rocks. The results are not straightforward because of a large recent magnetic overprint from the magnetic saw-blade, gutter and saw-table used at the drilling site for cutting the cores. Sites from the Hooggenoeg Complex show the best magnetic carriers and properties for a possibly (near)- primary signal, and these have been compared with other published data-sets from rocks of the same age. A conglomerate test on the Noisy conglomerates has shown that these rocks are very promising for future research on more samples. No clear correlation with (in situ) mean directions from this study and Biggin *et al.* (2011) is found, despite the fact that the rocks are comparable in the same complex and stratigraphic level. However, rocks from the Hooggenoeg Complex, including the intrusion, are the most likely candidates for carrying a (near-) primary component. Future work on these rocks must be stimulated to provide a more complete and better understanding of the geomagnetic behavior of Early Earth's core.

Acknowledgements

Funding for this study was received from the Molengraaff Fonds. Special thanks for Prof. Maarten de Wit from the African Earth Observatory Network (AEON) for funding the orientation of the cores and his hospitality during our stay in Cape Town. Prof. Cor Langereis gets a special note for his inspiring stories during the fieldwork and his help and mentoring during the rest of the project. Andy Biggin is thanked for his help and brainstorming during some discussion sessions on the results and Laura Roberts-Artal for her belief in further work on our rocks. The whole research group from 'The Fort' is thanked for their help, support and social talks.

References

Armstrong, R.A., Compston, W., de Wit, M.J., Williams, I.S., 1990. The stratigraphy of the 3.5 – 3.2 Ga Barberton Greenstone Belt revisited: a single zircon ion microprobe study. Earth Planetary Science Letters, vol. 101, 90-106.

Bennett, V.C., Nutman, A.P., Esat, T.M., 2002. Constraints on mantle evolution from $^{187}Os/^{188}Os$ isotopic compositions of Archean ultramafic rocks from southern West Greenland (3.8 Ga) and Western Australia (3.46 Ga). Geochimica et Cosmochimica Acta, vol. 66, no. 14. 2615-2630.

Biggin, A.J., Strik, G.H.M.A., Langereis, C.G., 2009. The intensity of the geomagnetic field in the late-Archaean: new measurements and analysis of the updated IAGA palaeointensity database. Earth Planets Space, vol. 61, 9-22.

Biggin, A.J., de Wit, M.J., Langereis, C.G., Zegers, T.E., Voûte, S., Dekkers, M.J., Drost, K., 2011. Palaeomagnetism of Archaean rocks of the Onverwacht Group, Barberton Greenstone Belt (southern Africa): potential geomagnetic reversals and evidence for the Vaalbara supercraton at ca. 3.5 Ga.

de Boer, C.B., 1999. Rock-Magnetic Studies on Hematite, Maghemite and Combustion-Metamorphic Rocks. Research thesis, Geologica Utraiectina, no. 177.

Butler, R.F., 1992. Paleomagnetism: Magnetic domains to geologic terranes.. Blackwell Scientific Publications.

Dankers, P.H.M., 1978. Magnetic Properties of Dispersed Natural Iron-Oxides of known Grain-size. Research thesis, University of Utrecht.

Dankers, P.H.M. & Zijderveld, J.D.A., 1981. Alternating field demagnetization of rocks,

and the problem of gyromagnetic remanence. Earth and Planetary Science Letters, vol. 53, 89-92.

Dunlop, D.J., 1982. Characteristic magnetic properties of (titano)magnetites in continental igneous rocks. Physics of the Earth and Planetary Interiors, 30, 273.

Fliegel, D., Kosler, J., McLoughlin, N., Simonetti, A., de Wit, M.J., Wirth, R., Furnes, H., 2010. In-situ dating of the Earth's oldest trace fossil at 3.34 Ga. Earth and Planetary Science Letters, vol. 299, Issue 3-4, 290-298.

Furnes, H., Staudigel, H., Thorseth, I.H., Torsvik, T., Muehlenbachs, K., Tumyr O., 2001d. Bioalteration of basaltic glass in the oceanic crust. Geochemistry, Geophysics, Geosystems, vol. 2.

Furnes, H., 2004. Early life Recorded in Archean Pillow Lavas. Science, vol. 304, 578.

Furnes, H. & Muehlenbachs, K., 2003. Bioalteration recorded in ophiolitic pillow lavas. *From:* Ophiolites in Earth History. Geological Society, London, Special Publications, vol. 218, 415-426.

Grosch, E.G., McLoughlin, N., de Wit, M. J., Furnes, H., 2009a. Drilling for the Archean roots of life and tectonic earth in the Barberton Mountains. Scientific Drilling 8, 24-28.

Grosch, E.G., McLoughlin, N., de Wit, M.J., Furnes, H., 2009b. Deciphering Earth's deep history: drilling in Africa's oldest Greenstone Belt. EOS 90, 350–351.

Heider, F. & Dunlop, D.J., 1987. Magnetic Properties of Hydrothermally Recrystallized Magnetite Crystals. Science, vol. 236, 1287-1290.

Hofmann, A., 2005. The geochemistry of sedimentary rocks from the Fig Tree Group, Barberton greenstone belt: Implications for tectonic, hydrothermal and surface processes during mid-Archaean times. Precambrian Research, vol. 143, 23-49.

Johnson, C.L., Constable, C.G., Tauxe, L., Barendregt, R., Brown, L.L., Coe, R.S., Layer, P., Mejia, V., Opdyke, N.D., Singer, B.S., Staudigel, H. and Stone, D.B., 2008. Recent investigations of the 0-5 Ma geomagnetic field recorded by lava flows. Geochemistry, Geophysics, Geosystems, 9(4).

Kamo, S.L. & Davis, D.W., 1994. Reassessment of Archean crustal development in the Barberton Mountain Land, South Africa, based on U-Pb dating. Tectonics, vol. 13, no.1, 167-192.

Knauth, L.P. & Lowe, D.R., 2003. High Archean climatic temperature inferred from oxygen isotope geochemistry of cherts in the 3.5 Swaziland Supergroup, South Africa. Geological Society of America Bulletin, vol. 115, 566-580.

Kröner, A., Hegner, E., Wendt, J.L., Byerly, G.R., 1996. The oldest part of the Barberton granitoid-greenstone terrain, South Africa: evidence for crust formation between 3.5 and 3.7 Ga. Precambrian Research, vol. 78, 105-124.

Letts, S., Torsvik, T.H., Webb, S.J., Ashwal, L.D., 2009. Paleomagnetism of the 2054 Ma Bushveld Complex (South Africa): implications for emplacement and cooling. Geophys. J. Int., vol. 179, 850-872.

Lowe, D.R. & Byerlee, G.R., 1999. Geological Evolution of the Barberton Greenstone Belt, South Africa. Geological Society of America, Special Paper, vol. 329.

McFadden, P.L. & McElhinny, M.W., 1988. The combined analysis of remagnetization circles and direct observations in paleomagnetism. Earth and Planetary Science Letters, vol. 87, 161-172.

McLoughlin, N, Brasier, M.D., Wacey, D., Green, O.R., Perry, R.S., 2007. On Biogenicity Criteria for Endolithic Microborings on Early Earth and Beyond. Astrobiology, vol. 7, no.1.

O'Nions, R.K. & Pankhurst, R.J., 1978. Early Archaean rocks and geochemical evolution of the Earth's crust. Earth and Planetary Science Letters, vol. 38, 211-236.

De Ronde, C.E.J., Kamo, S., Davis, D.W., de Wit, M.J. Spooner, E.T.C., 1991. Field, geochemical and U-Pb isotopic constraints from hypabyssal felsic intrusions within the Barberton greenstone belt, South Africa: Implications for tectonic and the timing of gold mineralization. Precambrian Research, vol. 49, 261-280.

Schoene, B., de Wit, M.J., Bowring, S.A., 2008. Mesoarchean assembly and stabilization of the eastern Kaapvaal craton: A structural-thermochronological perspective. Tectonics, vol. 27.

Shipunov, S.V., Muraviev, A.A., Bazhenov, M.L., 1998. A new conglomerate test in paleomagnetism. Geophys. J. Int., vol. 133, 721-725.

Stephenson, A., 1980a. A gyroremanent magnetization in anisotropic magnetic material. Nature, vol. 284, 49-51.

Stephenson, A., 1993. Three-Axis Static Alternating Field Demagnetization of Rocks and the Identification of Natural Remanent Magnetization, Gyroremanent Magnetization, and Anisotropy. Journal of Geophysical Research, vol. 98, 373-381.

Tessalina, S.G., Bourdon, B., Van Kranendonk, M., Birck, J. Philippot, P., 2010. Influence of Hadean crust evident in basalts and cherts from the Pilbara Craton. Nature Geoscience, vol. 3.

Thorseth, I.H., Furnes, H., Heldal, M., 1992. The importance of microbiological activity in the alteration of natural basaltic glass. Geochimica et Cosmochimica Acta, vol. 56, 845-850.

Usui, Y., Tarduno, J.A., Watkeys, M., HoComplexann, A., Cottrell, R.D., 2009. Evidence for a 3.45-billion-year-old magnetic remanence: Hints of an ancient geodynamo from conglomerates of South Africa. Geochemistry, Geophysics, Geosystems, vol. 10, no.9.

Viljoen, R.P. & Viljoen, M.J., 1969. An introduction to the geology of the Barberton granite-greenstone terrain. Geological Society of South Africa, Special Publication, vol. 9, 1-20.

de Vries, S.T., Nijman, W., Armstrong, R.A., 2006. Groth-fault structure and stratigraphic architecture of the Buck Ridge volcano-sedimentary complex, upper Hooggenoeg Complex, Barberton Greenstone Belt, South Africa. Precambrian Research, vol. 149, 77-98.

Walz, F., 2002. The Verwey transition – a topical review. Institute of Physics Publishing, vol. 14, 285-340.

Ward, J.H.W., 1999. The Metallogeny of the Barberton Greenstone Belt, South Africa and Swaziland. Geological Survey of South Africa.

Watson, G.S. & Beran, R.J., 1967. Testing a Sequence of Unit Vectors for Serial Correlation. Journal of Geophysical Research, vol. 72, no.22.

de Wit, M.J., Hart, R.A., Hart, R.J., 1987. The Jamestown Ophiolite Complex, Barberton mountain belt: a section through 3.5 Ga oceanic crust. Journal of African Earth Sciences, vol. 6, no.5, 681-730.